DOKUZ EYLÜL UNIVERSITY
GRADUATE SCHOOL OF NATURAL AND APPLIED SCIENCES

CYCLIC CHARACTERIZATION OF LOCKED AND STANDARD BRICK INFILLED REINFORCED CONCRETE FRAMES UNDER QUASI-STATIC LOADING CONDITIONS: EXPERIMENTAL AND ANALYTICAL WORK

by
Murat Arda UĞURLU

October, 2011
İZMİR

CYCLIC CHARACTERIZATION OF LOCKED AND STANDARD BRICK INFILLED REINFORCED CONCRETE FRAMES UNDER QUASI-STATIC LOADING CONDITIONS: EXPERIMENTAL AND ANALYTICAL WORK

A Thesis Submitted to the
Graduate School of Natural and Applied Sciences of Dokuz Eylül University
In Partial Fulfillment of the Requirements for the Degree of Master of Science
in Civil Engineering, Structural Engineering Program

by
Murat Arda UĞURLU

October, 2011
İZMİR

M.Sc THESIS EXAMINATION RESULT FORM

We have read the thesis entitled **"CYCLIC CHARACTERIZATION OF LOCKED AND STANDARD BRICK INFILLED REINFORCED CONCRETE FRAMES UNDER QUASI-STATIC LOADING CONDITIONS: EXPERIMENTAL AND ANALYTICAL WORK"** completed by **Murat Arda UĞURLU** under supervision of **Prof. Dr. Serap KAHRAMAN** and we certify that in our opinion it is fully adequate, in scope and in quality, as a thesis for the degree of Master of Science.

Prof. Dr. Serap KAHRAMAN

Supervisor

Yrd. Doç. Dr. Özgür ÖZÇELİK

(Jury Member)

Yrd. Doç. Dr. Selçuk SAATCI

(Jury Member)

Prof.Dr. Mustafa SABUNCU

Director

Graduate School of Natural and Applied Sciences

ACKNOWLEDGEMENTS

I would like to express my sincere gratitude to my supervisor Prof. Dr. Serap KAHRAMAN for her intelligent supervision, constructive guidance, inspiration and encouragement throughout the completion of this work. I also would like to express my special thanks to Researcher Dr. İ. Serkan MISIR, for sharing his experience in every stage of the thesis.

I would like to thank my tutors Assistant Prof. Dr. Özgür ÖZÇELİK and Prof. Dr. Türkay BARAN for their contributions to this study.

Also, I would like to express my appreciation for the support given by my colleagues in Earthquake and Structural Engineering Laboratory, especially by M.Sc. Sadık Can GİRGİN, Yıldıray SÖNMEZ and Serhan SARIDOĞAN.

Many individuals provided me with direct or indirect help during this study. In this respect I would like to thank my friends, E Ceren OCAK and Dr. A. Erdem KILAVUZ.

At last but not least, I would like to thank my father Osman UĞURLU, my mother Nafiye UĞURLU and my brother Emre UĞURLU for the support they provided me through my entire life.

Murat Arda UĞURLU

CYCLIC CHARACTERIZATION OF LOCKED AND STANDARD BRICK INFILLED REINFORCED CONCRETE FRAMES UNDER QUASI-STATIC LOADING CONDITIONS: EXPERIMENTAL AND ANALYTICAL WORK

ABSTRACT

Reinforced concrete frame structures with masonry infill walls constitute the significant portion of the buildings stock in Turkey. Therefore, it is very important to understand the behavior of masonry infill frame structures under earthquake loads. This study presents an experimental work performed on reinforced concrete (RC) frames with different types of masonry infills, namely standard and locked bricks. Earthquake effects are induced on RC frames by quasi-static test setup. Results obtained from different frames are compared with each other through various stiffness, strength, and energy related parameters. It is shown that locked bricks may prove useful in decreasing the problems related to horizontal and vertical irregularities observed in such structural systems, and moreover tests show that locked brick infills maintain their integrity up to very high drift levels, showing that they may have a potential in reducing injuries and fatalities related to falling hazards during severe ground shakings.

Keywords: Masonry infills; Reinforced concrete frames; Cyclic testing; Experimental methods; Earthquake engineering; Analytical modeling.

KİLİTLİ VE STANDART TUĞLA DUVARLI BETONARME ÇERÇEVELERİN QUASİ-STATİK YÜKLEME ALTINDA ÇEVRİMSEL TANIMLAMASI: DENEYSEL VE ANALİTİK ÇALIŞMA

ÖZ

Dolgu duvarlı betonarme çerçeveler Türkiye'deki binaların önemli bir kısmını oluşturmaktadır. Bundan dolayı, dolgu duvarlı betonarme çerçevenin deprem yükleri altındakini davranışını kavrayabilmek oldukça önemlidir. Bu tezde, farklı tiplerde dolgu duvarlı (geleneksel tuğla, kilitli tuğla) betonarme çerçevelerin deneysel çalışması anlatılmaktadır. Deprem etkileri betonarme çerçevelere quasi-statik yükleme ile etkitilmiştir. Farklı çerçevelerden alınan deney sonuçları birbirleriyle rijitlik, dayanım ve enerji sönümü gibi parametreler bazında karşılaştırılmıştır. Kilitli tuğlalı duvar sistemlerinin, bazı yapılarda gözlenen planda ve düşey doğrultudaki düzensizlik durumlarından doğan problemleri azaltabileceğine dair bulgular elde edilmiştir. Ayrıca testler, kilitli tuğlanın yüksek kayma değerlerinde bile bütünlüğünü koruduğunu ve deprem esnasında dolgu duvarın düzlem dışına yıkılmasından kaynaklanan olası yaralanmaların azaltılması konusunda bir potansiyele sahip olduğunu göstermiştir.

Anahtar Sözcükler: Dolgu duvar; Betonarme çerçeve; Çevrimsel yükleme; Deneysel metotlar; Deprem Mühendisliği, Analitik modelleme.

CONTENTS

Page

CHAPTER ONE
INTRODUCTION

1.1 General Information

The bare frames of reinforced concrete structures are filled with walls made by hollow clay bricks. These walls are often formed by fired clay bricks. Bricks are the oldest structural materials of the history. In designing procedure, the strength characteristics of infill wall materials assumed to be of no contribution except for its weight are not excessively emphasized [FEMA].

Infill wall has actually significant contributions to the behavior of the structure under earthquake and vertical loading, and the dynamic characteristics such as stiffness, bearing capacity, period, and damping [FEMA]. The reason for these contributions to be ruled out in the calculation and designing of structure is not only the fact that the strengths of infill wall materials are variable but also the fact that wall strengths are significantly affected by workmanship which is highly difficult to control. However, the characteristics of the infill walls are to be known in order to get familiar with the positive features of the infill walls which contribute to the behavior of the structure in reinforced concrete structures and in order to make use of them as much as possible or at least to avoid from their negative effects.

All of the walls in structures are shear walls under earthquake loads and just like all shear walls; they support horizontal loads until they reach their bearing capacity. In reinforced concrete framed structures, infill walls between columns have the strength of bearing horizontal loads, though limited. In the load levels below this limit, infill walls are shear walls with significant stiffness. When the limit is exceeded, the infill wall reaches its collapse failure and does not contribute to bearing anymore. Only the reinforced concrete frame resists the lateral loads.

Infill walls separate the volumes within the reinforced concrete frames and form the external cover of the buildings. Therefore, infill walls generally complete the openings of the reinforced concrete frame and form a plane enclosed by reinforced concrete columns and beams. The walls within the reinforced concrete frames are often preserved by the frame.

In this study, the effects of the standard brick and locked brick on the frame behavior will be analyzed in the light of the information given above.

1.2 Objectives and the Scope

It is very important to understand the behavior of masonry infill frame structures under earthquake loads. This study presents an experimental work performed on reinforced concrete (RC) frames with different types of masonry infill walls, namely standard and locked bricks which illustrated in Figure 1.1. To achieve an engineered infill frame, locked brick was used in the infill. It can slide longitudinally, but transversal sliding is restricted and increases the deformation capacity and decreases the strength deterioration. Locked brick has a potential of more structural energy damping during earthquakes with the use of different interface materials. It increases displacement capacity of frame without significant loss of integrity of infill. It is shown that locked bricks may prove useful in decreasing the problems related to horizontal and vertical irregularities observed in such structural systems, and moreover tests show that locked brick infill walls maintain their integrity up to very high drift levels, showing that they may have a potential in reducing injuries and fatalities related to falling hazards during severe ground shakings.

In this study, the contribution of infill materials to the frame strength mentioned in introduction, were tested with ½ scaled reinforced concrete frames whose characteristics will be given in the next section.

Reinforced concrete frame was tested with locked brick, standard brick and bare frame in 3 different tests and 4 pilot tests.

In order to represent reversed cyclic quasi-static load simulating an earthquake, a hydraulic cylinder with 0.3 mm/s velocity was used. After the same load was applied in three loops, the next value was applied.

In order to measure the deformations possible to occur during the experiments, strain gauges, string pots and LVDT’s were used. Data is recorded to a hard disc using data acquisition system and then was interpreted by the help of graphs and charts.

To conclude, structural contribution of two kinds of infill wall systems to the bare frame and the differences between these systems were aimed to reveal.

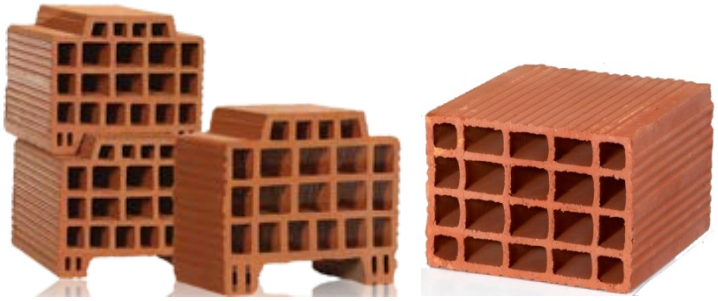

Figure 1.1 Locked brick and standard brick

CHAPTER TWO
LITERATURE REVIEW

Holmes (1961) investigated the behavior of infilled (brick and concrete) steel frames by using small-scale, single bay and single-story specimens. Numerical predictions for calculating the ultimate racking load and corresponding side sway deflection of infilled steel frames were carried out and compared with the test results. An equivalent diagonal strut model was used to model the wall panel. Horizontal load and deflections were calculated based on the strength of materials methods. The width of the equivalent strut was one third of the diagonal length (d/3). The comparison of the theoretical and experimental values revealed that the ultimate load predictions were in the range of 14% in regards to the majority. However deflection predictions scattered. Holmes stated that the formulas must be revised outside of the h/l=0.7~1.4 range. Moreover, openings in the brickwork infilling adversely affected the ultimate loads (leading to a 30%~40% drop at failure load).

Mallick and Severn (1967) proposed a new method by using finite element method tools based on a complementary energy. The effect of slip on the behavior was shown experimentally and included in the model as well as stress distribution along the contact lengths. A decrease in slip due to shear connectors increased the stiffness. Several tests on single-story and single-bay infilled steel frames were done to evaluate stiffness and strength values and compare them with the theoretical results. Failure was mostly due to the crushing of the infill material. Back to back arrangement or tandem method of testing was used for the infilled frames with span to height ratios of 1, 1.5 and 2. They found the method to be infeasible for multistory infilled frames.

Klingner and Bertero (1978) tested a one third scale sub-assemblage (1-1/2 bays wide and 3-1/2 stories high) of an 11 story building. Four specimens, one of which was a bare frame, were tested under reversed cyclic loading. Lateral load was applied at the top of specimens. The specimens were tested horizontally. Hollow core concrete and clay block units were bonded to the surrounding frame to obtain firm contact between the panel and the frame. Load controlled and displacement controlled types of loading were used. They drew several conclusions: load-

displacement graphs of the infilled specimens showed pinching behavior and a sudden drop in the strength due to a decrease in the infill wall resistance. The behavior of infilled frames was improved in terms of stiffness at service levels, strength and energy absorption and dissipation capacity. Klingner and Bertero (1978) believed that positive effects of the engineered infill walls suppressed the disadvantages created by increased inertial forces due to changes in stiffness and period values. Adding infill walls decreased P-Δ effects and the risk of incremental collapse due to high energy dissipation through the hysteric behavior. The writers compared the experimental results with the numerical ones obtained from macro modeling of the specimens based on equivalent strut concept. Tensile strength of the struts was relatively low due to low tensile strength of the infill material and low contribution of panel steel. Although bond-slip behavior was not included in the model, the results were quite good because the behavior of the infill wall determined the behavior of infilled frame.

Gülkan and Wasti (1993) investigated the nonlinear behavior of one bay-one storey reinforced concrete frames with different storey heights using finite element methods and they have concluded that ignoring the effect of masonry infilled walls inside frames in the calculation of the natural periods of structures can be erroneous. Frame modeled with elastic column-beam elements while infill wall modeled with two dimensional isoparametric elements. Infill wall material which can be at different heights, accepted to behave according to Mohr-Coulomb failure criteria. Force displacement relationship which determines frame stiffness, researched under increasing lateral loading. The results showed that infill wall start to effect frame behavior if its height more than one of three. Column shear force increases 4 or 5 times than given values of calculations which regard only bare frame. Lastly, they noted that full infilled frame behavior is different from partial infilled frame behavior.

Mehrabi, Shing, Schuller & Noland (1996) examined the effect of infill walls on the seismic performance of reinforced concrete frames. Two types of frame specimens, one of which represented older structures, were examined. Aspect ratios (h/l) were 1/1.5 for strong frames and 1/1.5 and 1/2 for weak frames. Solid and

hollow core concrete units were used as infill materials. 12 one half scale single-bay, single-storey specimens, one of which was bare frame, were tested under either cyclic or monotonic loading. The columns had continuous reinforcement. Distribution of vertical loads, loading history (load or displacement controlled for cyclic loading), and height to span ratio, frame type, and infill type were among the variables. They stated that failure and frame panel interaction was governed by relative strengths of the panel and the frame. Ultimate load ratios with respect to the bare frame for weak frame infilled with hollow solid concrete units were 1.5 and 2.3 respectively. Those values for ductile infilled frames with respect to the ductile virgin frame (the capacity of the virgin frame was calculated as 14 5kN) were predicted as 1.4 and 3.2 respectively. Hysteretic energy dissipation of solid infilled frames was better than that of hollow infilled frames both for weak and strong frames. The increase in span to height ratio increased the ultimate loads about 10 % for strong infill walls and 17% for weak infill walls. Mehrabi et al. (1996) believed that this observation may be wrong if changes in aspect ratio resulted in different failure mode. Vertical load distribution between frame and panel did not affect the load carrying capacity. However, a 50% increase in vertical load increased stiffness 30% and lateral load capacity 25% for solid concrete infilled weak frames with aspect ratio of ½. Shear failure of the columns, generally seen in specimens with weak frames and strong infill walls, obstructed the development of an effective load resisting mechanism was observed in the solid concrete infilled ductile frames. Moreover presence of strong infill walls decreased the drift levels which shear cracks was observed with respect to the specimens with weak infill walls.

Mosalam, White & Gergely (1997) examined unreinforced solid concrete masonry infilled gravity load designed steel frames under quasi-static cyclic lateral loads. The number of bays, relative material strengths of concrete units and mortar joints, and opening area size and configuration, were investigated parameters. 5 single story, ¼ scale specimens were tested up to failure. Mosalam et al. (1997) drew several conclusions: failure shifted from corner crushing to mortar cracking when relative strength of concrete blocks and mortar joints increased. Failure mode changed the ultimate load approximately 20%. However, presence of window opening did not change ultimate loads significantly. The width of equivalent strut

was not uniform; it decreased towards the loaded corners. They proposed a hysteresis model with physically meaningful parameters based on test results.

Sahota & Riddington (1998) showed that using a copper-tellurium lead layer increased the cracking load of the tested infill but neither changed the ultimate strength so much nor had any adverse effect on the cracking performance of the infilled frame. The lead layer was attached to the underside of the top beam of the frame, using a contact adhesive prior to the construction of the infill. They tested three half-scale square masonry infilled steel frames. The masonry infill was formed from three hole perforated clay engineering bricks. The frames were formed from Grade 43 steel. The frames were formed of steel rather than reinforced concrete because the method used to simulate the shortening of the columns as a result of shrinkage and creep put the columns into tension. They concluded that the inclusion of a lead layer in an infilled frame structure will reduce significantly the compressive load that is transferred onto the infill as a result of column shortening and in the tests undertaken, the inclusion of the copper–tellurium lead layer did not have any adverse effect on the racking performance of the infilled frame.

Crisafulli, Carr & Park (2000) proposed an approach using the principles of capacity design, a new design approach is proposed for cantilever infilled frames, in which the ductile behavior is achieved by controlled yielding of the longitudinal reinforcement at the base of the columns. A pre-cracked connection is induced between the infilled frame and the foundation, where plain round dowels can be placed to control shear sliding. The proposed procedure also assures a simple evaluation of the lateral resistance, avoiding the uncertainties associated with the complexity of the panel-frame interaction. The use of tapered beam-column joints with diagonal reinforcement is recommended in order to reduce the opening of the joints and to improve the transfer of the lateral forces from the frame to the masonry panel.

Marjani and Ersoy (2002) investigated the seismic behavior of masonry infilled reinforced concrete frames by an experimental program composed of six one bay-two storey frames. The experimental results showed that using clay hollow brick infill increased both the strength and stiffness values compare to their bare frame

counterparts. They stated that structural frames are often filled with masonry walls serving as partitions or as cladding. Although infill walls usually are not considered in the structural design, their influence on the behavior of the frame is considerable. Up until the infill walls cracks, the contribution of the infill to both lateral stiffness and strength is very significant. The infill also changes the dynamic characteristics of the frame. The change in lateral stiffness, strength and natural period of the frame structure due to the presence of infill walls change the behavior of the building under seismic action.

Aref & Jung (2003) proposed a new infill panel, composed of polymer matrix composite (PMC) material. The PMC infill wall system consisted of two fiber-reinforced polymer laminates with an infill of vinyl sheet foam. At the interface between the laminates, viscoelastic honeycomb is used to dissipate energy and improve the damping characteristics of the structure. As part of this research, analytical and experimental studies were performed to explore the effectiveness of this seismic retrofitting strategy and to examine the behavior of the PMC-infill wall system when subjected to monotonic and cyclic loading. The optimal design for the stacking sequence of a PMC-infill wall panel was determined based on the performance and material cost using the finite-element analysis. It was shown that the introduction of a PMC infill wall in a semi-rigidly connected steel frame produced significant enhancements to the stiffness, strength and energy dissipation.

Moghadam (2004) introduces a new analytical approach for the evaluation of shear strength and cracking pattern of masonry infill panels. This method is based on minimizing the factor of safety with reference to the failure surfaces. This approach can also be used to determine the shear strength parameters and the modulus of elasticity of brickwork material. The paper also presents the results of experimental and analytical investigations on repaired and strengthened brick infilled steel frames. Two main repair techniques were examined in which the corner material is replaced with concrete or a concrete cover is placed on the panel. Both experiment and analysis have confirmed the efficiency and adequacy of these techniques.

Taher and Afefy (2008) presented a comparison between nonlinear analysis for reinforced concrete frame with masonry infill panels modeled as a whole and infill panels modeled as unilateral diagonal struts where each strut activated only in compression. The system is composed of a homogenized continuum for the reinforced concrete members braced with unilateral diagonal struts for each bay, which are only activated in compression. Identification of the equivalent system characteristics and nonlinear material properties is accomplished from the concepts of inverse analysis, along with statistical tests of the hypotheses, employed to establish the appropriate filtering scheme and the proper accuracy tolerance. The results of this study showed the significance of infill walls in increasing the strength, stiffness, and frequency of the entire system depending on the position and amount of infill walls.

D'Ayala, Worth & Riddle (2009) used two different numerical modeling techniques, and comparing results with experimental evidence, this paper sets out to identify the range of the various parameters that influence masonry infill concrete frame interaction. Their aim is to provide a more realistic model for the lateral load redistribution between infill and frame in the post cracking regime, and to quantify relative values of stiffness, capacity and ductility which lead to brittle shear failure of the system. The methodology that they used to model shear behavior in both the commercial Algor v19.3 analysis package and the open source Drain 3DX program is first set forth. Similar progressions of shear failure were demonstrated in both modeling approaches. The main discrepancies between the models are with respect to the localized lateral displacements at the nodes where shear failure has been identified though these do not vary in orders of magnitude. Notwithstanding the slight differences between the outputs of the two programs, they both highlight the importance of accurately simulating shear failure capacity in columns if the correct failure pattern and load capacity of infilled frames are to be reliably predicted.

Mohammadi & Akrami (2010) presented a paper of the results of an experimental investigation on some engineered infilled frames with high ductility and adjustable strength. To achieve an engineered infilled frame, an element is added to the infill, called Frictional Sliding Fuses (FSFs). The fuse acts before infill corner crushing and

controls the infill so that it is not overloaded. Consequently, it increases the deformation capacity and decreases the strength deterioration. An FSF has a frictional nature, based on which the infill has more appropriate hysteresis cycles, leading to more structural energy damping during earthquakes. The results show that the engineered infilled frames have adjustable strength, as well as high ductility and damping.

Past research work has shown that the infill masonry walls induce significant change in the seismic response of reinforced concrete frames. Effects of masonry walls are in general positive meaning that masonry infill walls increase overall stiffness and strength of reinforced concrete frames. On the negative side, masonry infill walls may induce torsional motion due to in-plan irregularities, and soft-storey and short column effects due to vertical irregularities.

CHAPTER THREE
EXPERIMENTAL STUDY

3.1 Introduction

In order to conduct an experimental analysis of the behaviors of locked brick infilled frame (LBF), standard brick infilled frame (SBF) and bare frame (BaF) under reversed cyclic static load (quasi-static loading), 7 reinforced concrete frames were produced and tested in the testing apparatus (as it is illustrated in Figure 3.1) in Dokuz Eylül University Civil Engineering Department, Earthquake and Structural Engineering Laboratory. 4 of these frames were used for pilot tests. In these pilot tests some of experimental faults were observed and these faults were improved in the other 3 tests. Reinforced concrete frames were produced, taking the laboratory environment into consideration, as single bay, single storey with locked bricks and standard bricks in a scale of ½. These specimens designed according to the Turkish Earthquake Code, 2007 and modeling techniques of this code were used (Ministry of Public Works and Settlement, 2007).

3.2 Test Variables

Under the reversed cyclic quasi-static loading, two different types of brick infill materials were used: standard brick and locked brick respectively in the second and the third experiments. The first experiment was tested with a bare frame. The information about the bricks that were used will be given in the following sections.

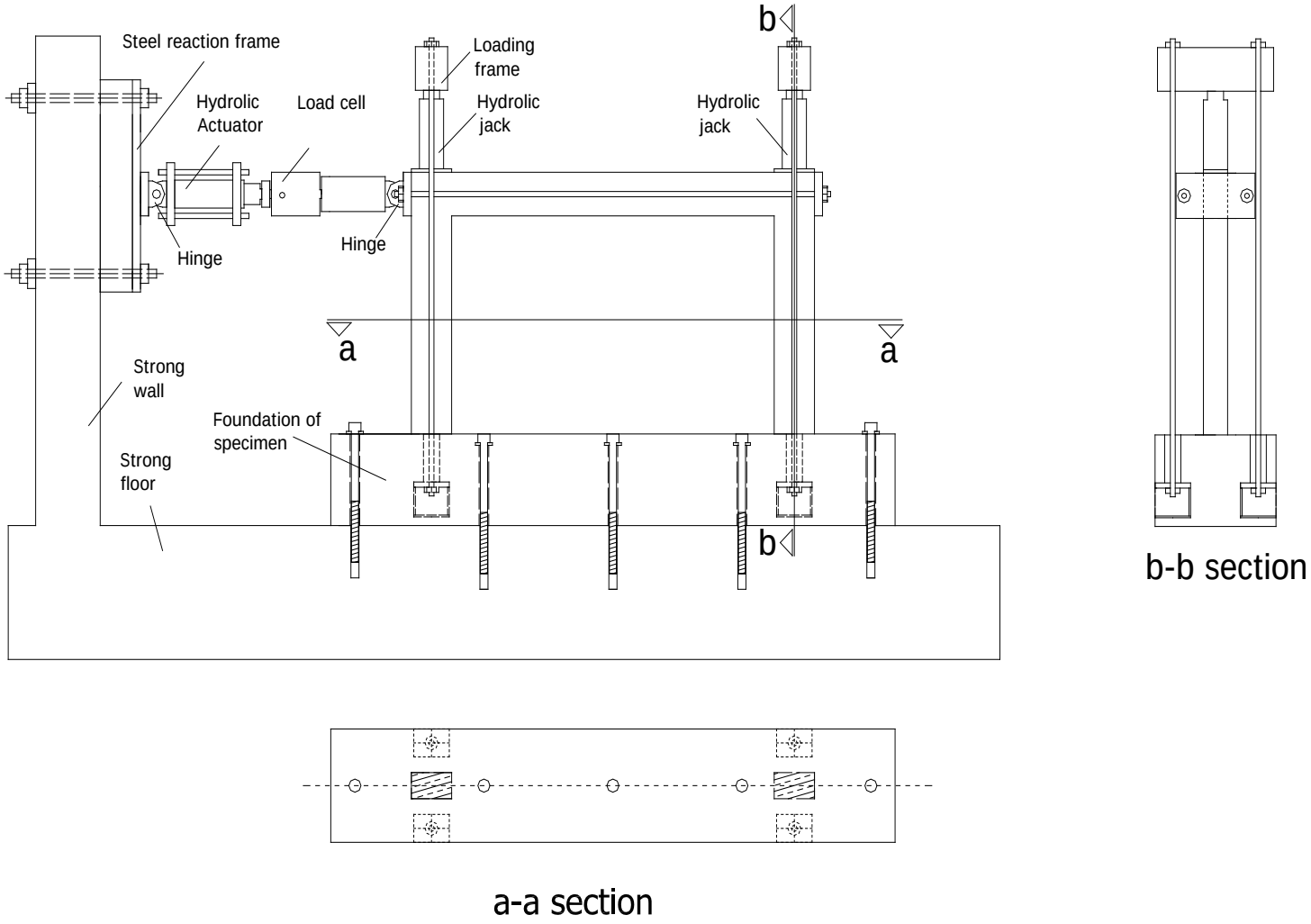

Figure 3.1 Test set-up

3.3 Details of the Specimens

3.3.1 Reinforced Concrete Frame

The sizes of the reinforced concrete frame and its foundation are shown in Figure 3.2. Reinforcement details and dimensions of all test specimens are the same. The dimensions of the columns and beams are 250x150 mm and the dimensions of the foundation are 250x150 mm.

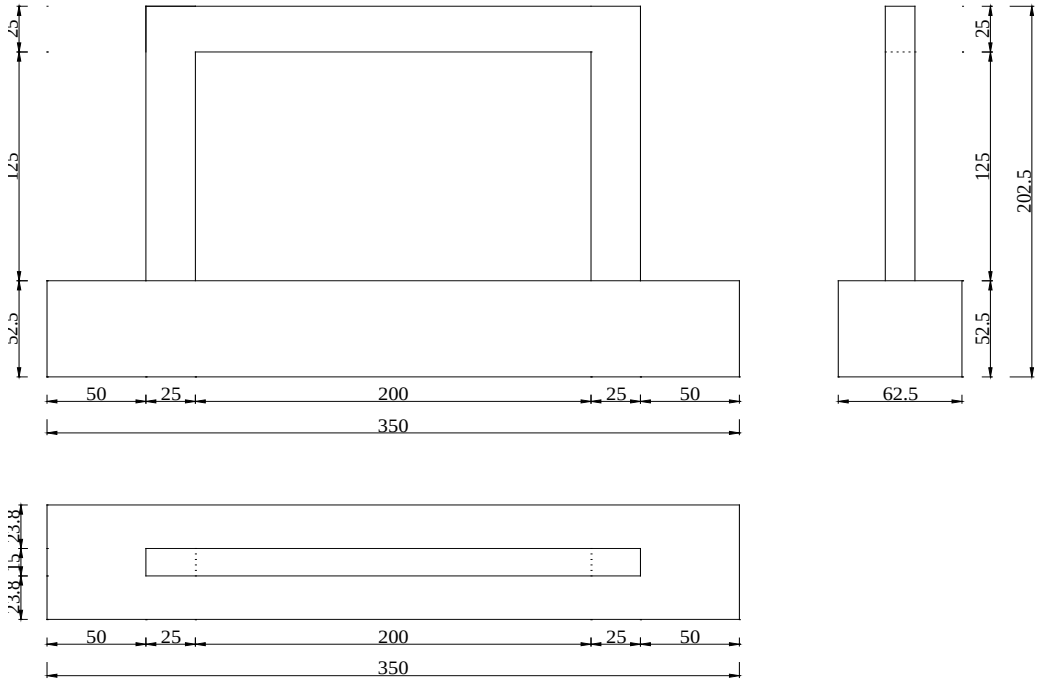

Figure 3.2 Lateral, top and front views of reinforced concrete frame (the units are cm.)

Deformed bars with the diameter of 12 mm and 10 mm were used as longitudinal reinforcements for columns and beams respectively. Deformed bars with the diameter of 16 mm were used for foundation. Stirrups were used in column end region with the length of 70 mm interval, in column middle zone with the length of 90 mm interval and 8 mm diameter, in beams with the length of 90 mm interval and 8 mm diameter, in foundation end region with the length of 85 mm interval, in foundation middle zone with the length of 100 mm interval and 8 mm diameter. Reinforcement details of reinforced concrete frame showed in Figure 3.3-5

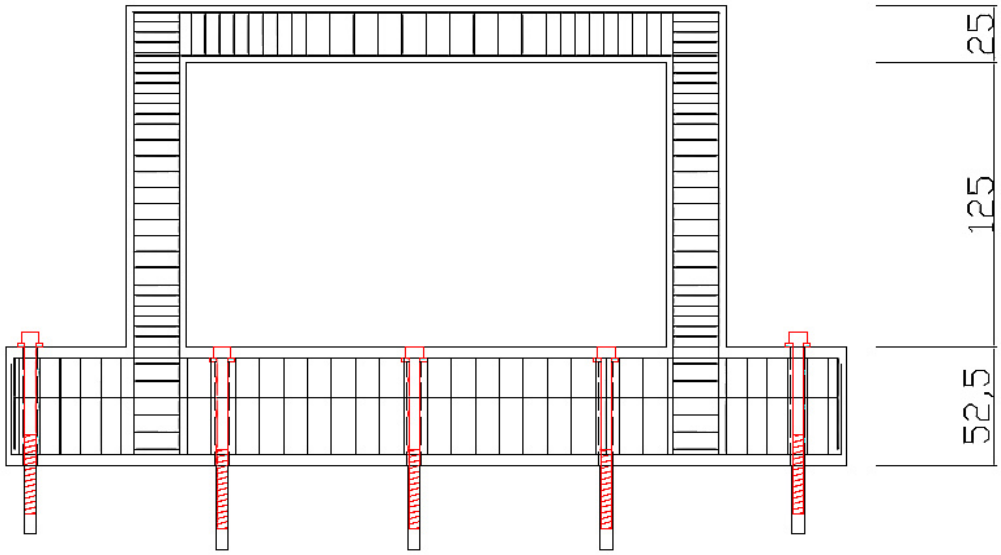

Figure 3.3 Detailing of transverse reinforcement (the units are cm.)

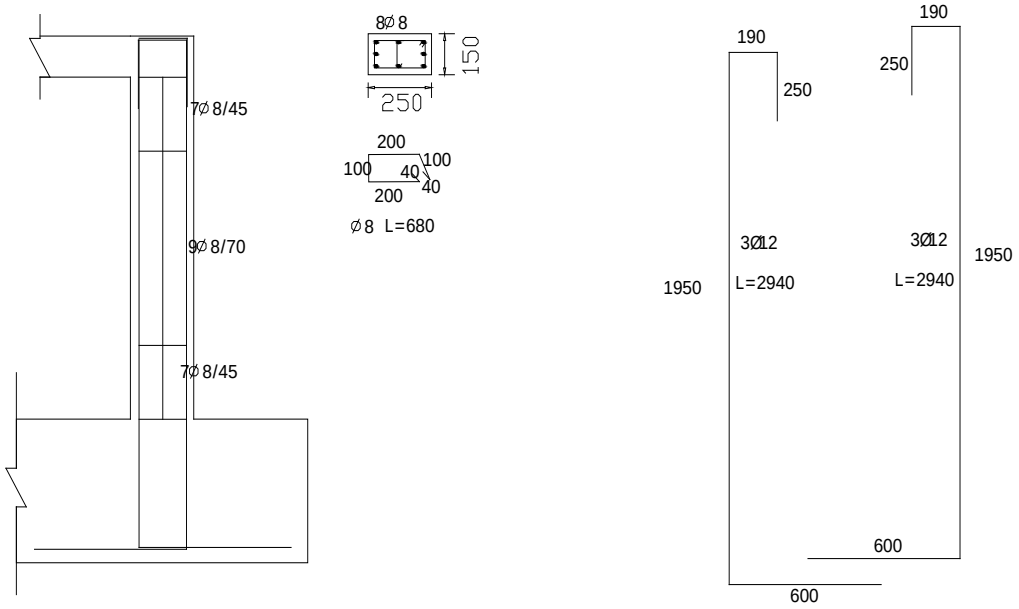

Figure 3.4 Detailing of column reinforcements (the units are mm.)

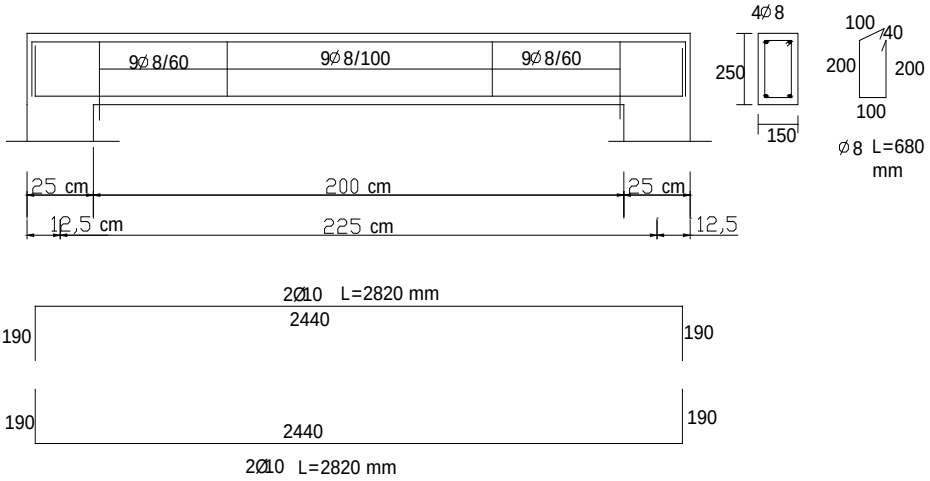

Figure 3.5 Detailing of beam reinforcements

3.3.2 Locked Brick

Locked brick which was developed by Vardarlı Toprak Sanayi and Ticaret A.Ş. was used in the 3rd test to demonstrate the affects of behavior of reinforced concrete frame. The size of the brick which was produced specifically with a scale of ½ is 12 cm wide, 12.5 cm long and 6.75 cm high (Figure 3.6).

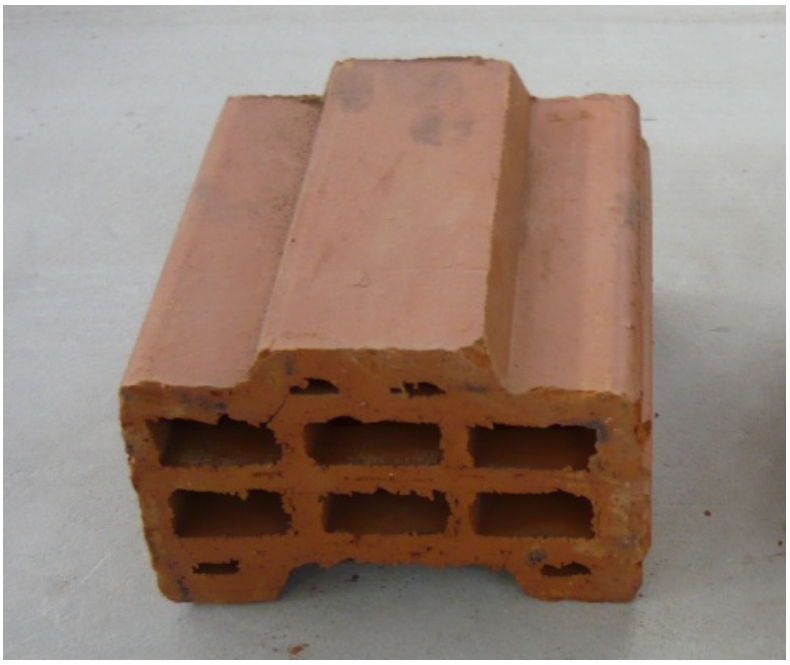

Figure 3.6 Locked brick with a scale of ½

Locked brick infilled frame (LBF) which is developed by using locked brick may have some advantages when compared to standard brick infilled frame (SBF):

- The most important difference of LBF is the time and the cost saved during construction, besides the shape and sizes of the locked brick.
- All masonry workers know how to construct locked brick wall; furthermore, there is no need to make an extra ground implementation before construction unlike standard wall system. In LBF, mortar has to be used only for the first and the last row (upper beam and column contact zone). Mortar is by no means used in the other zones.
- What is more, it can also be stated that beam molds are possible to use after the wall construction with LBF

The following steps are followed for LBF:

i. First of all a string was drawn from column to column with the help of traditional methods
ii. Mortar was used for only the first row of bricks as illustrated in Figure 3.7
iii. Extra attention was paid during the impletion of the brick's female part
iv. Interspacing between the bricks during construction was carefully avoided.
v. There was neither mortar nor chemical cohesive used between brick lanes.
vi. Except for the first row, all bricks were placed on the subjacent male parts of the bricks as illustrated in Figure 3.8.
vii. All rows were constructed by the help of plumb line and in vertically balanced.
viii. Polyurethane foam was used between the last row and the beam as illustrated in Figure 3.9
ix. After the infill wall construction procedure, the wall was conventionally mortared both from inside and outside.

Figure 3.7 First row of locked bricks

Figure 3.8 Locked brick usage during construction

Figure 3.9 Polyurethane foam

3.3.3 Standard Brick

Within the scope of the 2nd test which was to demonstrate the effects of the standard brick on the reinforced concrete frame, standard brick which was exclusively produced with a scale of ½ was used and its sizes are: 11.5 cm wide, 12 cm long and 6.5 cm high (Figure 3.10).

The following steps are followed for SBF:

i. First of all, a string was drawn from column to column by using traditional methods and some mortar was coated on the mating surfaces of bricks to bricks and to frames, just like in LBF(Figure 3.11)
ii. Interspacing between the bricks during construction was carefully avoided.
iii. All rows were constructed by the help of plumb line and in balance, and construction was completed.

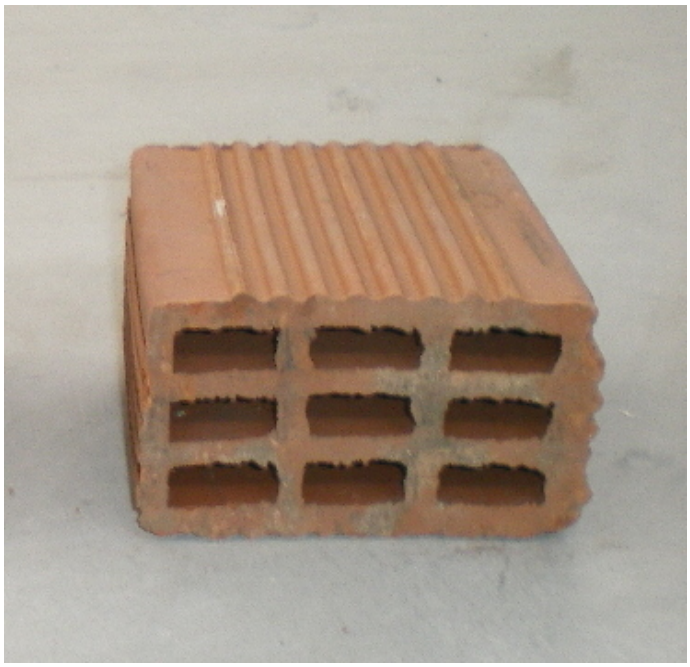

Figure 3.10 Standard brick with a scale of ½

Figure 3.11 Standard brick construction

3.4 Test Set-up and Instrumentation

The test specimens were attached to the strong floor and loaded until failure. Horizontal and vertical loadings were independently applied throughout the test. Test set up consisted of a steel reaction frame to apply the vertical load, 4 hydraulic rams, 2 of them for axial loading of each columns and the other 2 for restrain the movement of foundation, 4 pumping equipment to apply the axial loading, 2 loading frames, a load cell, a displacement controlled hydraulic actuator attached to the steel reaction frame, and a data acquisition system (DAQ). Test set-up is shown in Figure 3.1.

3.4.1 Strain Gauge (SG)

3.4.1.1 General

One of the instrumentations to be used in experimental studies in which the earthquake behaviors of the RC buildings are simulated and joint beam-column reinforced concrete frames are used is strain gauges which set cross-section properties and accordingly, possible outcomes to be developed in relevant components as seen in Figure 3.12.

Strain gauges which system are illustrated in Figure 3.13 are formed by a plastic film layer at the bottom, metallic foil resistor (3-6 μm) in the middle, and a laminated film layer (15-16 μm) at the top. Strain gauge elongates or shrinks with the material that it is firmly stuck to. Elongation or shrinkage in the folio layer causes changes in the electrical resistor. How much an object is strained is obtained by means of this resistance change.

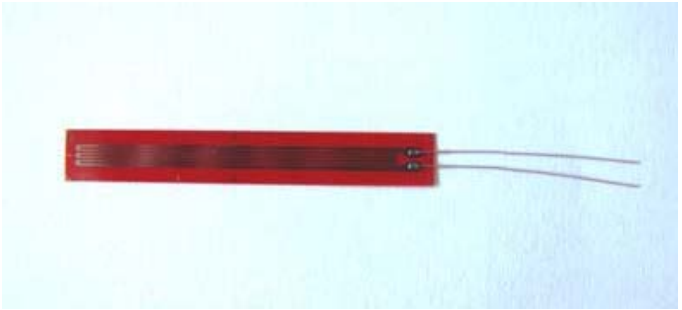

Figure 3.12 Strain gauge

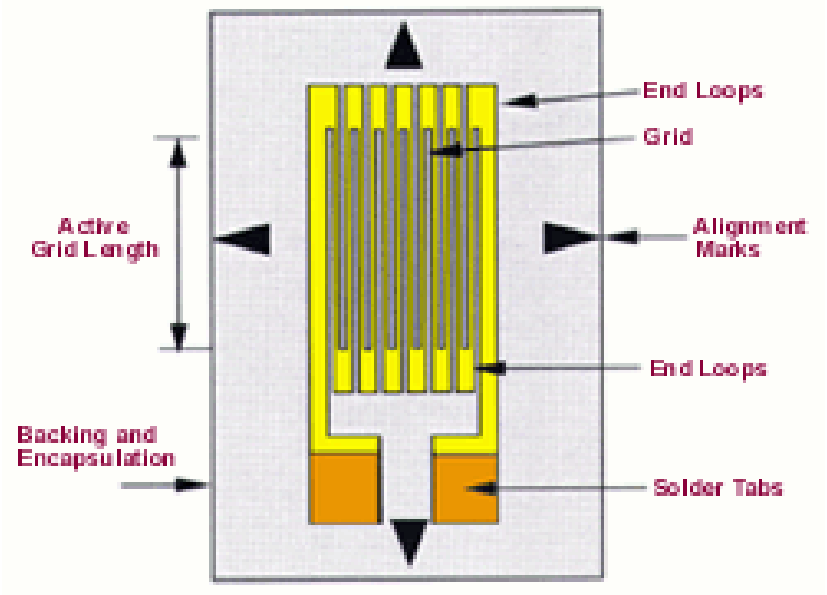

Figure 3.13 The strain gauge system (Coope, n.d.)

Before starting the strain gauge process, the convenient spots are detected and these spots are grinded and sandpapered until a smooth surface is obtained, then they are cleansed with alcohol. Strain gauge is treated with adhesive and pressure is applied for a while by sticking the strain gauge to the spot that it is to be applied. It is important to apply the pressure with a piece of nylon to avoid adhesive contagion.

TML brand and FLA 10-11 type strain gauges with 120 ohm were used in the project. 16 strain gauges process in total were executed to the reinforcements in the zones that could be critical within each frame. A total of 8 strain gauges being under the two columns and two at each side (right and left), a total of 4 strain gauges being at the column beam joints and one at each side, and a total of 4 strain gauges being on top and bottom of the beams were used in Figure 3.14, the reinforcements to which strain gauge process is applied are illustrated.

Figure 3.14 Reinforcements were applied strain gauge

3.4.1.2 Strain Gauge Application

Within the scope of the project, prefabricated production factory was visited, before concreting, for the strain gauge process of the reinforced frame. Firstly, the spots that strain gauges to be fixed were marked for the process as illustrated in Figure 3.15. Then, for a cleansed surface was needed, these spots were grinded and sandpapered which seen in Figure 3.16. Moreover, the terminals which facilitate the transmission of the electrical changes to data acquisition system were soldered to the strain gauges as illustrated in Figure 3.17. In order to verify the fact that strain gauges work properly, they were tested with a 120 ohm voltmeter.

After cleansing the sandpapered reinforcements with alcohol, strain gauge application started. Strain gauges and terminals which were soldered to each other were fixed to the marked spot with a tape. After the surfaces of the strain gauges were fully coated with adhesive, they were fixed to the marked spots of the reinforcements and pressure was applied for a while as seen in Figure 3.18 and 19.

Applied strain gauges were controlled with voltmeter one more time in order to see whether there is no malfunction as illustrated in Figure 3.20. Strain gauges which

could not reach 120 ohm were removed and substituted. Connecting cables which transmit data to data acquisition system from strain gauges were soldered to terminals; this is available to see in Figure 3.21. After concreting, cables were tagged in order to provide clear understanding of which strain gauge is connected to which cable. Cables which come from two different columns were formed into a single line which illustrated in Figure 3.22 and taken out from the middle section where the shear force zone of the beam is not high.

In order to protect strain gauges from water affect which was caused by fresh concrete, SB Tape was applied on it. SB Tape, which is a pasty material, is applied, by hand, to cover the strain gauge and terminal without leaving any space. Furthermore, during concreting, SB tape was covered by araldite in order to prevent mechanical impacts of the aggregate. Araldite is, similarly, a pasty material and applied on SB tape with a tea spoon.

Because the desiccation of araldite takes a day, concreting was postponed to the next day. To prevent the strain gauges from any damage while concreting, vibration was processed outside the mold.

Figure 3.15 Marking

Figure 3.16 Grinding

Figure 3.17 Soldering

Figure 3.18 Adhesive

Figure 3.19 Application of pressure

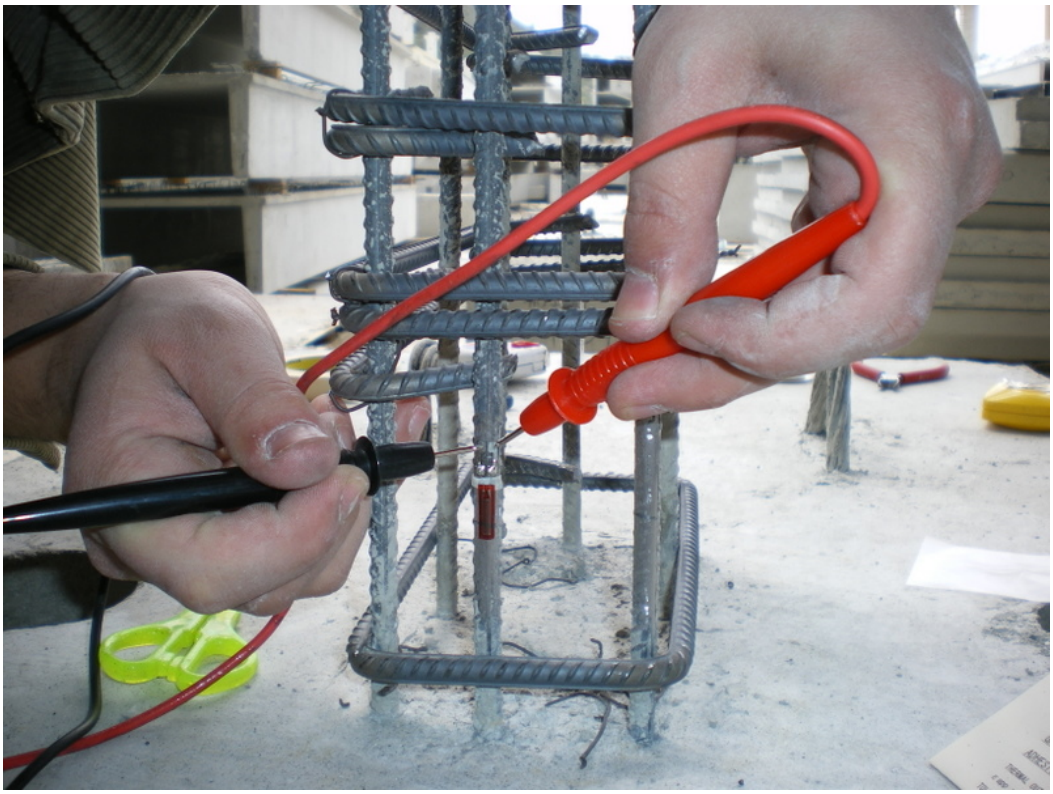

Figure 3.20 Checking

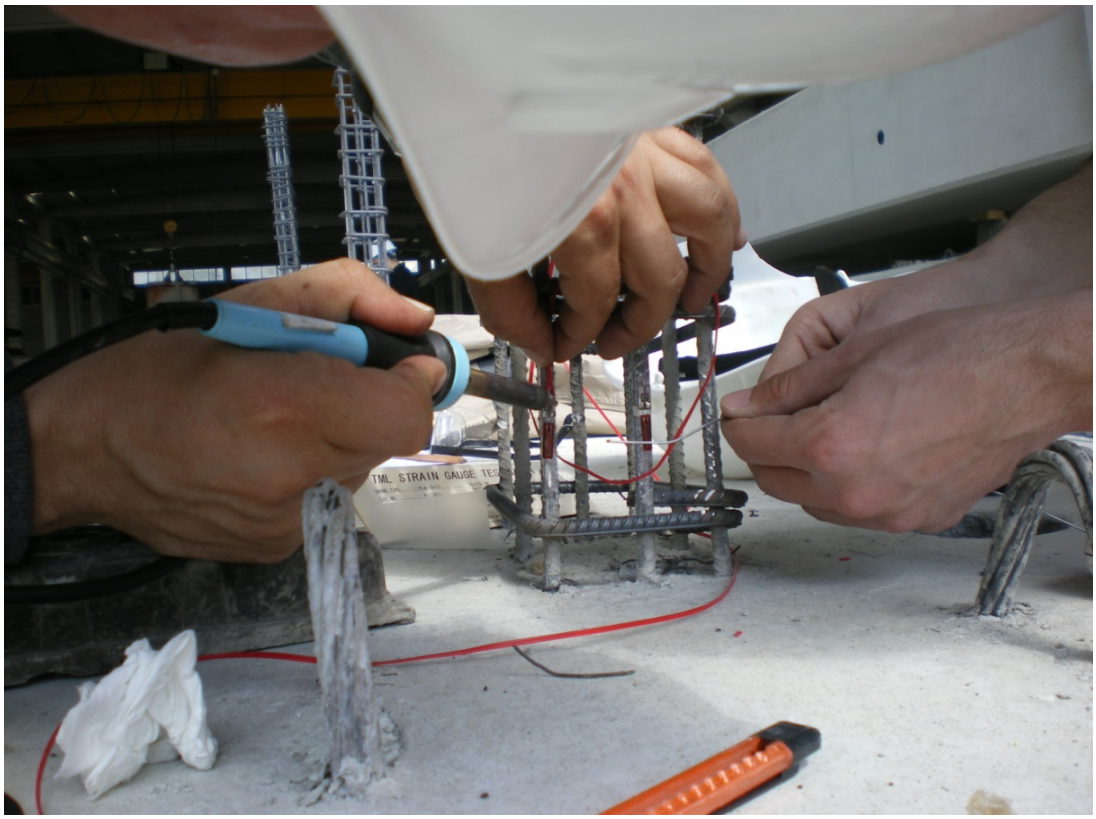

Figure 3.21 Soldering of terminals

Figure 3.22 Forming of connecting cables

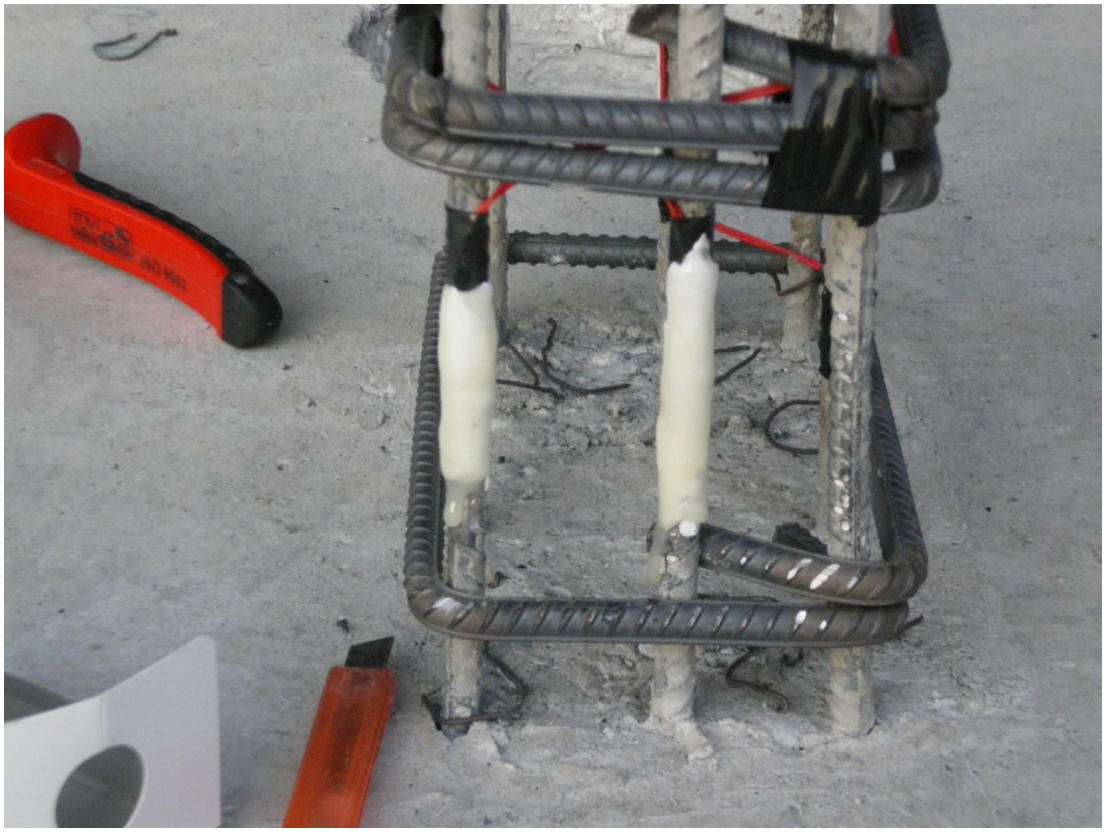

Figure 3.23 Strain gauges at final state

3.4.2 Placement and Fixing of Specimens

When the test set up preparations were finished, the specimens were brought to Dokuz Eylül University Civil Engineering Department, Earthquake Engineering and Structural Laboratory. The Specimens were taken down from their hooks which were placed in two edges of the foundation. If present, the blanks between the foundation and the laboratory floor which are caused by the curvilinear foundation base after the setting of the concrete were filled with metal sheets. Afterwards, the foundation beam was vertically fixed to the laboratory ground with 5 high strength studs as it is illustrated in Figure 3.24. In addition to the studs, 10 tons of forces each were vertically loaded onto the foundation axis with hydraulic rams on both sides in order to minimize the movement of the foundation which seen in Figure 3.25.

After the attachment of the foundation to the laboratory ground, infill wall construction was started according to the specimen type. SBF and LBF were implemented within the 2nd and the 3rd tests respectively. After the construction process, both walls were mortared as illustrated in Figure 3.29. After the locked brick was constructed in the 3rd test, filet was applied between mortar and the infill, as it is illustrated in Figure 3.27, in order for the impact of the locked brick on mortar cracking to be observed. As it mentioned before, the 1st specimen was tested without infill wall. In order to observe the crack formation more transparently, both sides of the frame and, if present, infill wall were engrained with lime. In an attempt to define the locations of the cracks formed during the test according to a reference point and to see where the cracks are after the test, grids with 12.5 cm space in between were drawn after the exsiccation of the lime as seen in Figure 3.30. These grids are specified with numbers vertically and letters horizontally.

After completion of the fixation of the reinforced concrete frame and, if present, construction of infill wall, placement of the loading equipment was started.

There are two steps for the placement process of the loading equipment: The first step is the placement of axial loading equipment (Figure 3.31) which represents the structural loads and the second step is the placement of horizontal loading equipment (Figure 3.32) which represents earthquake.

The head piece which is formed by plates welded to each other and is shown in Figure 3.31 was slung with a crane, and the studs were bind with washers and nuts in such a way that one edge of the stud with one and remaining free. Before the placement of the hydraulic ram which helps the vertical loading to be applied, a metal plate was used in order to transmit the vertical load properly to the column, and this metal plate was equilibrated with a water gauge. The parts of frame which were unsuitable to the scale were sandpapered until they were balanced. After the hydraulic ram was placed, the head piece which was slung with crane and studs were placed on top of the hydraulic ram and the other edges of studs were socked. The socked edges of the studs were tightened with washers and nuts. Finally, a little pressure was applied on the hydraulic ram in order to prepare the loading for the implementation. This process is also followed for the other column in the very same way.

In the second step, the hinge plate was connected to the hydraulic ram and neared to the column till it touched the column surface. Being slung with a crane, base plate was neared to the surface of the other column. The plate was merged with studs and tightened with nuts.

Figure 3.24 Studs

Figure 3.25 Hydraulic rams which constrain foundation

Figure 3.26 Locked brick infilled frame

Figure 3.27 The filet

Figure 3.28 Standard brick infilled frame

Figure 3.29 Mortared infill

Figure 3.30 Gridding

Figure 3.31 Axial loading equipment (hydraulic ram)

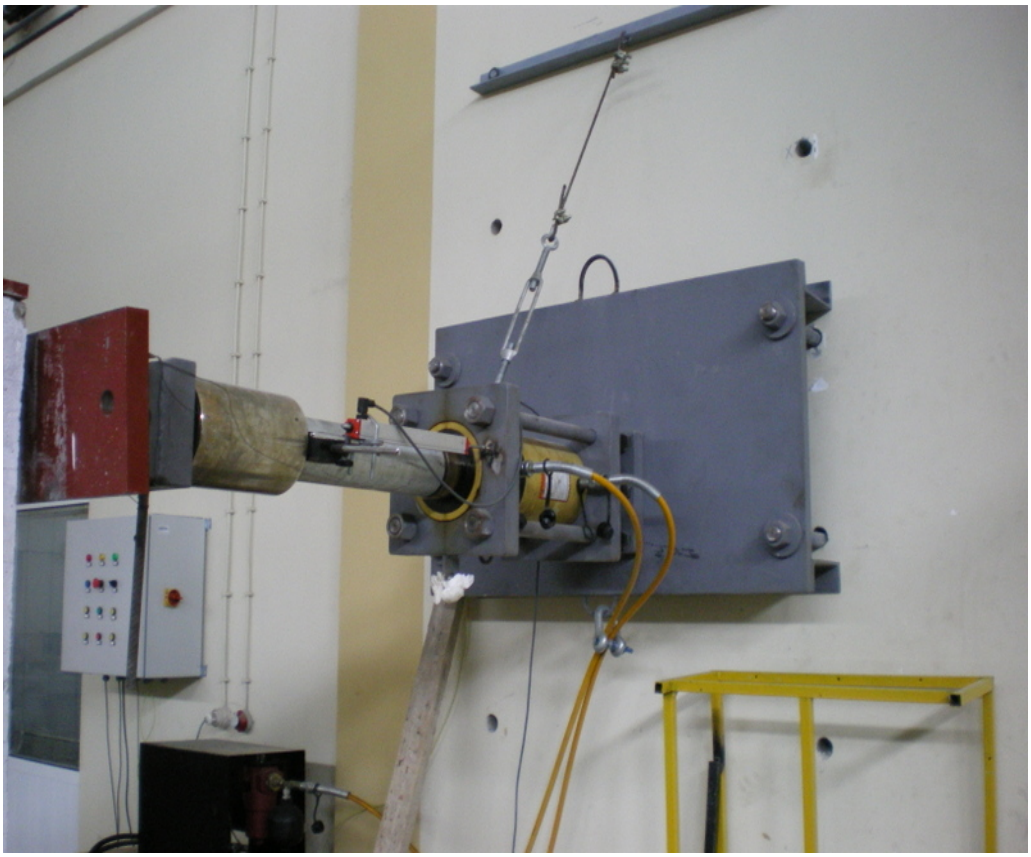

Figure 3.32 Horizontal loading equipment (actuator)

3.4.3 Placing of the Sensors and the Data Acquisiton System

In the scope of the project, displacements and strains of reinforcements in frame, structural elements, infill wall and critical zones which appeared during the test had been foreseen. For this purpose, strain gauge application for strains of reinforcements was represented in section 3.4.1.2. In this section, LVDTs and string pots which measure structural materials will be discussed.

Strain gauges and LVDT-type instrumentations, which have already been mentioned, are used in determining the system behavior with cross-section properties and hence, possible outcomes to be developed in relevant components for the experimental studies in which the earthquake behaviors of the reinforced concrete buildings are simulated and joint beam-column reinforced concrete frames are used. In frame type specimens, monitoring the horizontal displacements on floor level, in-plane and out-of-plane movements of the foundation and the specimen, reading the torsion values of critical column zones and recording the diagonal deformation

values of infill walls are completed by the means of displacement gauge LVDT (Linear Variable Differential Transformers) (Figure 3.33).

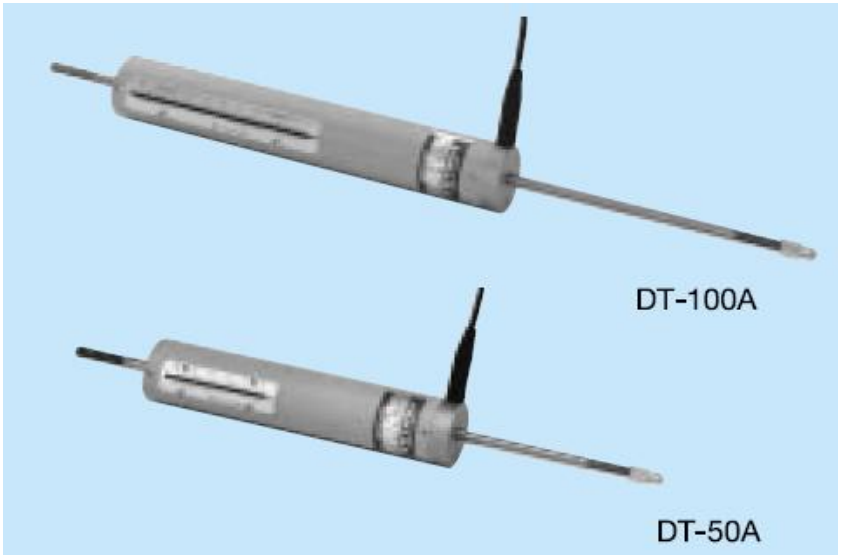

Figure 3.33 Linear variable differential transformer (LVDT)

Kyowa brand and DT-100A and DT-50A type LVDTs were used in tests. LVDTs are named in accordance with the displacement they measure. In the scope of the project, 9 LVDTs with 100 mm long and 1 LVDT with 50 mm long were used. The number of LVDTs and their intended use were illustrated in Table 3.1.

Some points to consider about LVDTs are;

- Using it must be avoided in places which are affected by vibration.
- On high level of displacements, it takes a while to observe a steady LVDT.
- Except for the elongation-shrinkage direction, LVDTs should not be exposed to displacements.

LVDTs, which were mentioned above, and their lay-out on frame and the given displacements in order to specify their position on test set up were given in Figure 3.34 for the 2nd and the 3rd tests and in Figure 3.35 for the 1st test.

Table 3.1 Placement of LVTDs and their capacities

LVDT	Placement of LVDTs	Capacity (mm)
12	Vertical Movement of The Right-Side of The Foundation	100
13	Load Cell	100
17	Actuator Displacement	100
22	Horizontal Movement of The Foundation	100
23	Vertical Movement of the Left-Side of The Foundation	100
24	Horizontal Movement of The Right Column	100
25	Horizontal Movement of Left-Side of The Left Column	100
26	Horizontal Movement of Right-Side of The Left Column	100
27	Horizontal Movement of Left-Side of The Right Column	100
28	Horizontal Movement of Right-Side of The Right Column	50

Before placing the LDVTs to the frame, pre-specified spots were marked on the frame. Marked spots were drilled with a drill bit of 10 mm wide and anchors were placed. By putting silicon the external peripheries of the anchors, movement of anchors were prevented. Then, clamps which fasten up LDVTs were placed. Plexiglas was stabilized with silicon in a leveled fashion to the places where the rods of LVDTs touched on the frame (Figure 3.36). Therefore, the points to be measured were rendered stable. LVDTs were fixed by clamps and their evenness was monitored by spirit level. LVDTs which were placed parallel to the ground floor were anchored with footed magnet which is illustrated in Figure 3.37.

Diagonals of infill wall were drawn for the placement of string pots and the points were marked where the string pots were to be placed. The points were drilled where string pot and its spring fix, and put silicon placing the anchors. Lastly, the string pots were fastened with screws.

In order to observe the lateral movement of the frame, the system which can be seen in Figure 3.39 was set. Dial gage was placed with a footed magnet on lateral direction.

Data obtained from LVDTs, string pots and strain gauges were transmitted with hyperlink cables to data acquisition system. Which channel of data acquisition system is used to connect LVDTs and string pots is shown in Table 3.1. Finally, data acquisition system was connected to the computer with a USB cable.

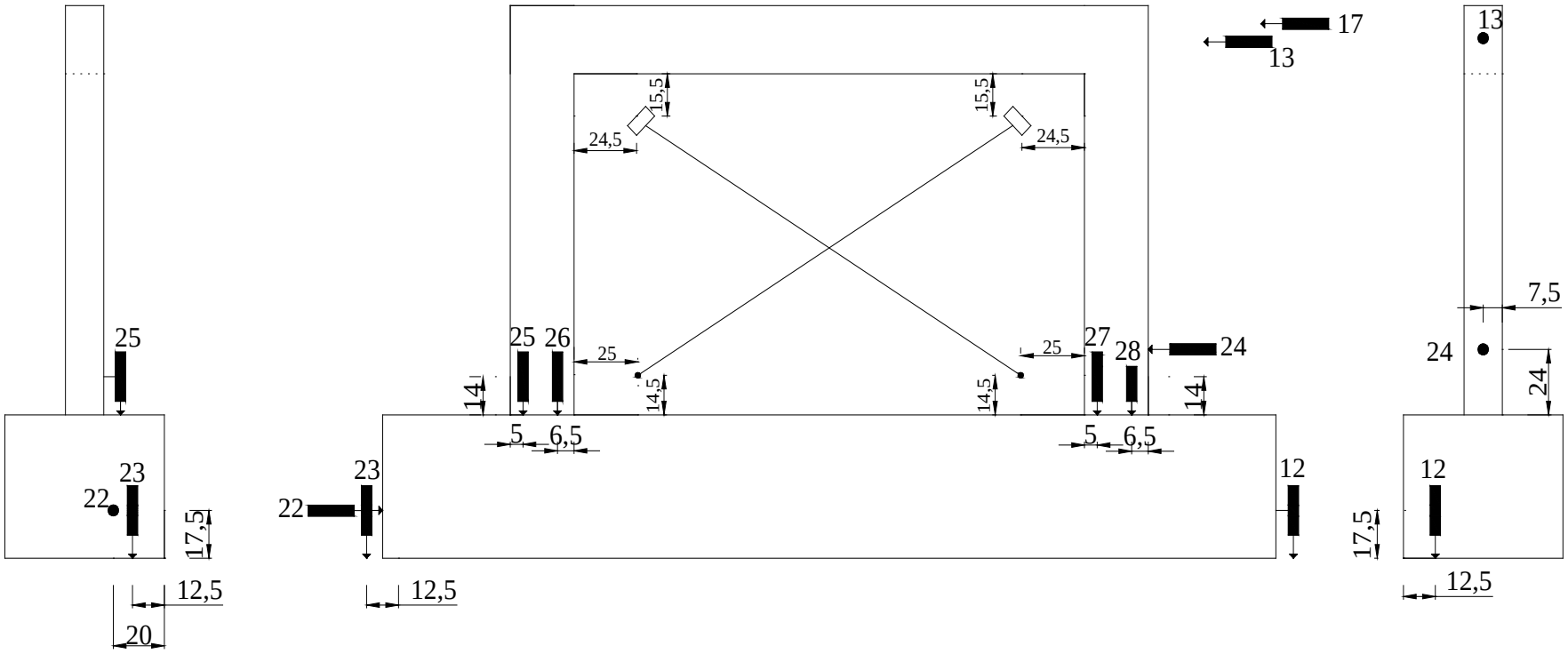

Figure 3.34 LVDT and string pot placement for specimen 2 and 3 (units are cm.)

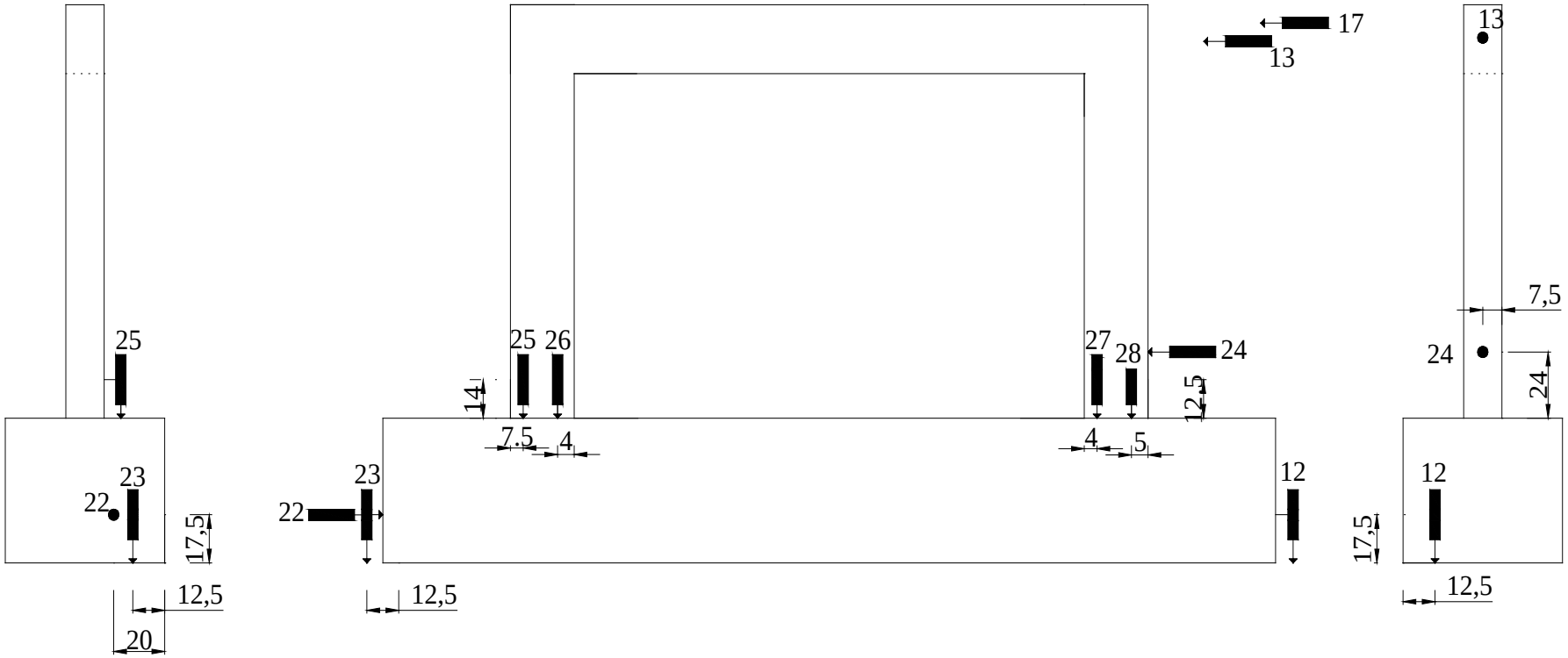

Figure 3.35 LVDT placements for bare frame (units are cm.)

Figure 3.36 Silicon application

Figure 3.37 Settled LVDT

Figure 3.38 LVDT with magnetic base

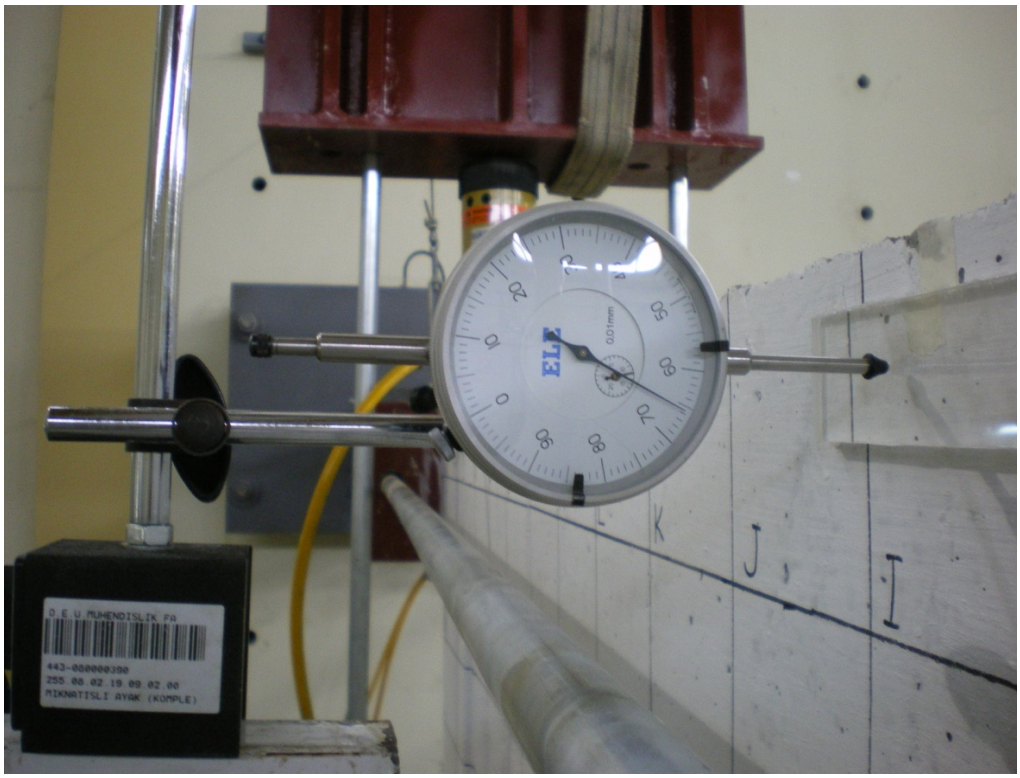

Figure 3.39 Dial gage

Figure 3.40 Control panel of actuator

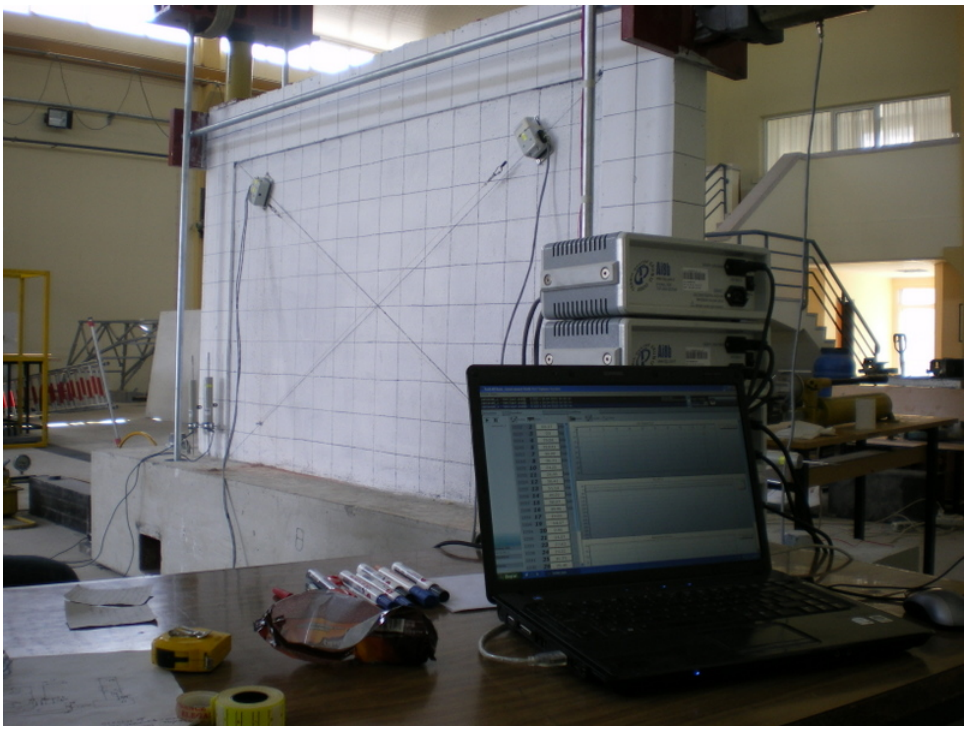

Figure 3.41 Data acquisition system and computer

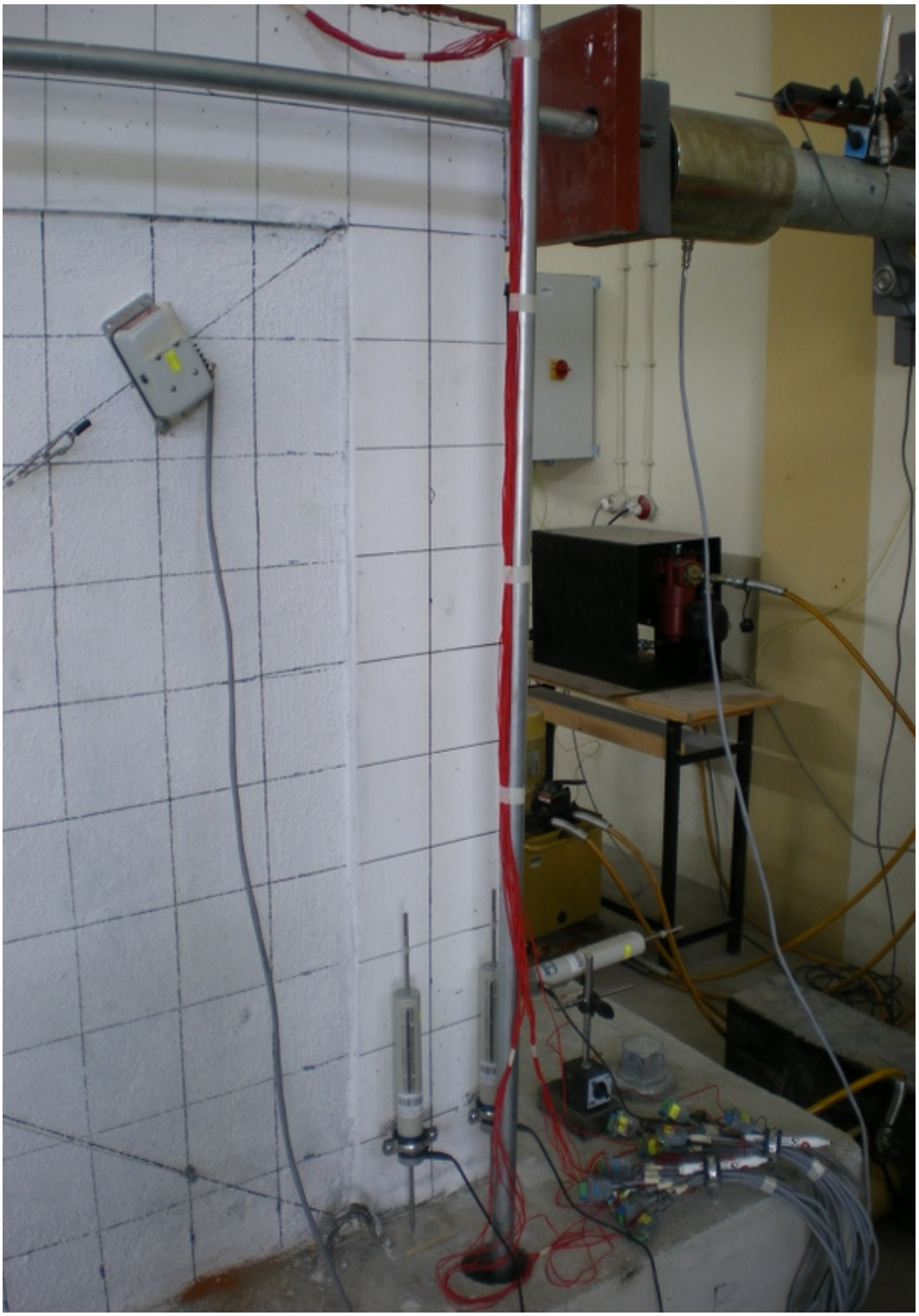

Figure 3.42 Connecting cables of LVDTs, string pots and strain gauges

3.5 Test Procedure

There are some important procedures that have to be applied before starting the test and after the placement of the test specimen and instrumentation. Setting up loading protocol and installing it to the testing program, calibration of the strain gauges, string pots and LVDTs and setting testing programs are some of the most important procedures. These procedures are going to be analyzed in this section.

Setting up displacement loading protocol is conditional upon the roof drift. Displacement loading protocol was determined according to ACI T1.1-01 (American Concrete Institute [ACI], 2001). Firstly, before testing, actuator was brought closer to the frame till it touches the top part of it. The point that it touches is taken as the starting position.

The loading is applied in 3 cycles. A positive displacement value (push) is applied in the first step. Subsequently, twice of this value is applied in the negative direction (pull). Finally, the system is brought back to starting position. That is to say, the system is pushed and pulled in equal values. Every single pushing and pulling process is called “loading step”. This process is applied for 3 times for a displacement value and then, next displacement value starts. Each of these processes is called *cycle*. Every cycle has 6 loading steps.

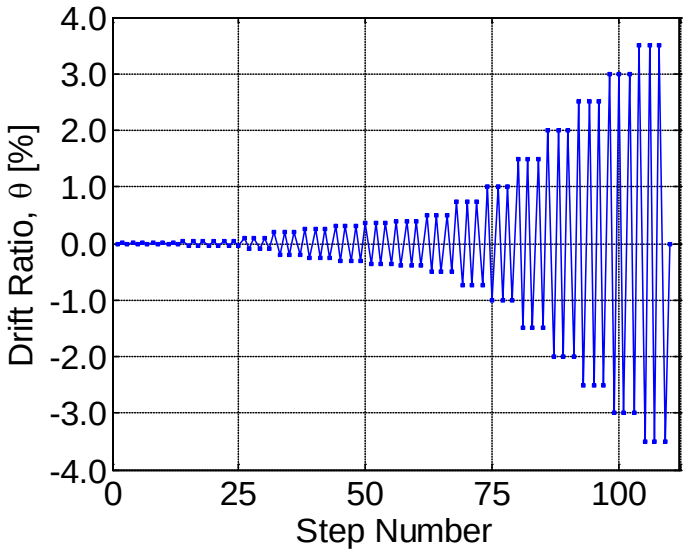

Figure 3.43 Load pattern

CHAPTER FOUR
TEST RESULTS

Total of eighteen target displacement cycles with three full cycles at each target displacement were imposed to the frames in each test. In all the tests, the applied maximum story drift was 3.5%. In the following sections some general and detailed observations regarding the results are presented.

4.1 Bare Frame (BaF)

Bare frame specimen was designated as the reference frame in order to compare its response against infill specimens. Displacement controlled (DC) type of loading was applied to this specimen. The total axial load applied to the each column was approximately 10% of axial load capacity of columns, 84 kN and kept constant throughout test. Maximum applied load was 100.9 kN for the forward cycle.

The first flexural cracks were observed at a story drift of 0.28%. The restoring force corresponding to this drift was measured to be 35.8 kN. In the first cycle of the 12^{th} target displacement corresponding to a drift level of 0.56%, the first time yielding of the longitudinal reinforcement was recorded. At this drift level, the restoring force was measured 57.3 kN. Base shear – top drift diagram of BaF is seen in Figure 4.1.

The asymmetry of hysteresis curve of bare frame arises from some little mistakes during testing.

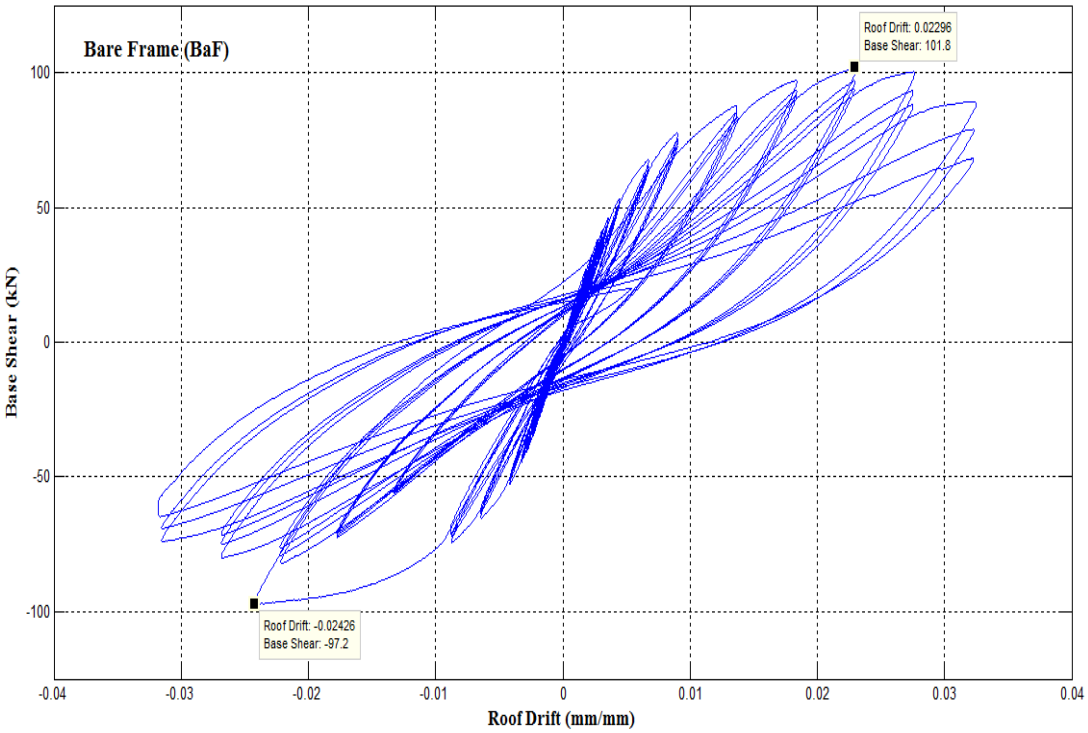

Figure 4.1 Base shear – top drift diagram for bare frame

Figure 4.2 Final form of bare frame at the final state

Table 4.1 Maximum loads and corresponding displacements for bare frame

Specimen: Bare Frame (BaF)				
Cycle No.	Corresponding Displacement Δmax @ Pmax (mm)	Maximum Load Pmax (kN)	Corresponding Displacement Δmax @ Pmax (mm)	Minimum Load Pmax (kN)
1	0.33	337	0.23	198
2	0.45	473	0.18	124
3	0.49	519	0.15	85
4	0.57	624	0.08	-8
5	0.80	883	-0.13	-236
6	1.43	1542	-0.80	-879
7	2.75	2769	-2.10	-2219
8	3.39	3288	-2.78	-2862
9	4.10	3877	-3.51	-3533
10	4.66	4237	-4.26	-4156
11	5.34	4671	-4.86	-4532
12	6.68	5428	-6.23	-5345
13	10.11	6922	-9.67	-6654
14	13.54	7941	-36.39	-9908
15	20.56	8961	-19.95	-5694
16	27.58	9914	-26.62	-7379
17	34.44	10378	-33.31	-8386
18	41.40	10233	-40.29	-8146
19	48.72	9097	-47.26	-7534

4.2 Standard Brick Infilled Frame (SBF)

Standard brick infill frame was designated as comparison frame in order to compare its response against locked brick infill frame. The total axial load applied to the each column was approximately 10% of axial load capacity of columns, 84 kN and kept constant throughout test. Maximum applied horizontal load was 137.4 kN for the forward cycle.

The first damage was observed when the infill wall separated from the beam at a drift level of 0.20%. The corresponding restoring force at this drift level was 96.3 kN. The first flexural cracks were observed at a story drift of 0.34%. The corresponding restoring force was measured 116.2 kN. At the first cycle of the 12^{th} target displacement corresponding to a drift level of 0.67%, the first time yielding of

the longitudinal reinforcement was recorded. At this drift level, the restoring force was measured to be 129.0 kN. Base shear – top drift diagram of SBF is seen in Figure 4.3.

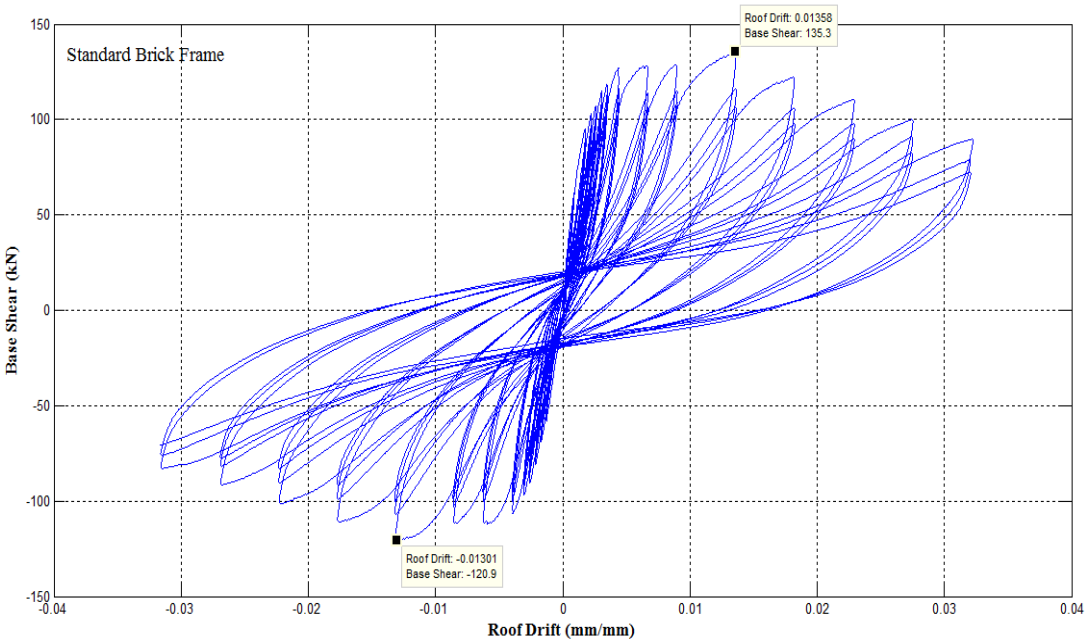

Figure 4.3 Base shear – top drift diagram for standard brick infilled frame

Figure 4.4 Final form of standard brick frame at the final stage

Table 4.2 Maximum loads and corresponding displacements for bare frame

Specimen: Standard Brick Frame (SBF)				
Cycle No.	Corresponding Displacement Δmax @ Pmax (mm)	Maximum Load Pmax (kN)	Corresponding Displacement Δmax @ Pmax (mm)	Minimum Load Pmax (kN)
1	0.39	2157	0.30	1793
2	0.38	2401	0.28	1662
3	0.43	2700	0.26	1495
4	0.55	3277	0.17	813
5	0.68	3815	0.03	-19
6	1.34	6288	-0.64	-2103
7	2.67	9711	-1.94	-5926
8	3.38	10479	-2.53	-7022
9	3.90	10890	-3.20	-8266
10	4.61	11707	-3.91	-9253
11	5.23	12071	-4.57	-9854
12	6.60	12951	-5.91	-10869
13	9.87	13053	-8.85	-11403
14	13.26	13103	-12.54	-11376
15	20.29	13796	-19.47	-12321
16	27.22	12481	-26.37	-11322
17	34.33	11285	-33.35	-10334
18	41.22	10209	-40.18	-9331
19	48.28	9151	-47.36	-8448

4.3 Locked Brick Infilled Frame (LBF)

Locked brick infill frame was designated as comparison frame in order to compare its response against standard brick infill frame. Displacement controlled type of loading was applied to this specimen. The total axial load applied to the columns was approximately 10% of axial load capacity of columns, 84 kN and kept constant throughout test. Maximum applied horizontal load was 97.5 kN for the forward cycle.

The first damage was observed when the infill wall separated from the beam at an inter-story drift level of 0.20%. The corresponding restoring force at this drift level was 55.8 kN. The first flexural cracks were observed at an inter-story drift of 0.35%.

The corresponding restoring force was measured 68.6 kN. At the first cycle of the 12th target displacement corresponding to a drift level of 0.75%, the first time yielding of the longitudinal reinforcement was recorded. Base shear – top drift diagram of LBF is seen in Figure 4.5.

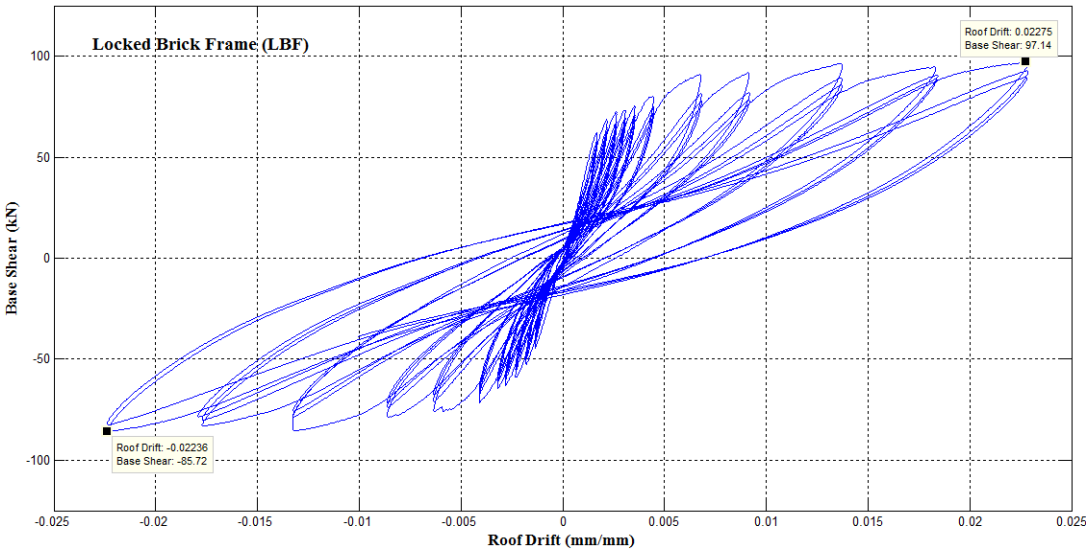

Figure 4.5 Base shear – top drift diagram for locked brick infilled frame

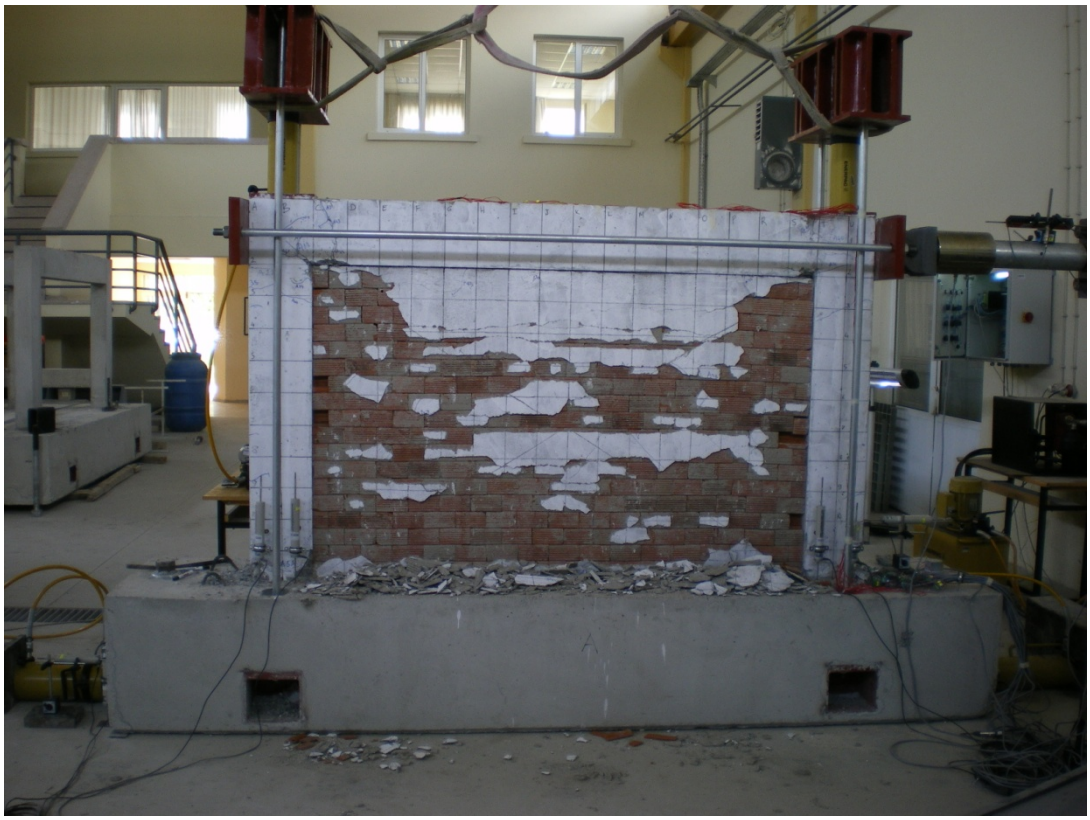

Figure 4.6 Final form of locked brick frame at the final stage

Table 4.3 Maximum loads and corresponding displacements for bare frame

Specimen: Locked Brick Frame (LBF)				
Cycle No.	Corresponding Displacement Δmax @ Pmax (mm)	Maximum Load Pmax (kN)	Corresponding Displacement Δmax @ Pmax (mm)	Minimum Load Pmax (kN)
1	0.33	337	0.23	198
2	0.45	473	0.18	124
3	0.49	519	0.15	85
4	0.57	624	0.08	-8
5	0.80	883	-0.13	-236
6	1.43	1542	-0.80	-879
7	2.75	2769	-2.10	-2219
8	3.39	3288	-2.78	-2862
9	4.10	3877	-3.51	-3533
10	4.66	4237	-4.26	-4156
11	5.34	4671	-4.86	-4532
12	6.68	5428	-6.23	-5345
13	10.11	6922	-9.67	-6654
14	13.54	7941	-36.39	-9908
15	20.56	8961	-19.95	-5694
16	27.58	9914	-26.62	-7379
17	34.44	10378	-33.31	-8386
18	41.40	10233	-40.29	-8146
19	48.72	9097	-47.26	-7534

Table 4.4, summarizes observed damage states of the walls and structural system and corresponding force levels; in addition to these, first yielding of the reinforcing bars and observed maximum lateral load levels are also documented.

Table 4.4 Damage states at different drift ratios and corresponding force levels for all specimens

Specimen	First separation			First diagonal crack			First flexural cracks			First yielding			Concrete spalling			Observed max. lateral load	
	Drift [%]	Load [kN]		Drift [%]	Load [kN]		Drift [%]	Load [kN]		Drift [%]	Load [kN]		Drift [%]	Load [kN]		Drift [%]	Load [kN]
BaF	-	-		-	-		0.28	35.8		0.56	57.3		2.00	93.0		2.50	100.9
SBF	0.20	96.3		0.40	120		0.34	116.2		0.67	129.0		2.00	107.3		1.50	137.4
LBF	0.20	55.8		0.25	67.8		0.35	68.6		0.75	85.2		2.00	84.4		3.00	97.5

Figure 4.10-4.17 show the states of standard brick frame (SBF) and locked brick frame (LBF) specimens at different drift ratios for visual damage comparison on the infill walls. At high drift ratio levels, it is particularly apparent that locked brick frame specimen suffers considerably less infill damage. At the end of the test at 3.5% drift ratio, bricks in the locked brick frame specimen remained almost intact and only plaster cracks were observed whereas in the standard brick frame specimen many bricks were lost due to diagonal forces.

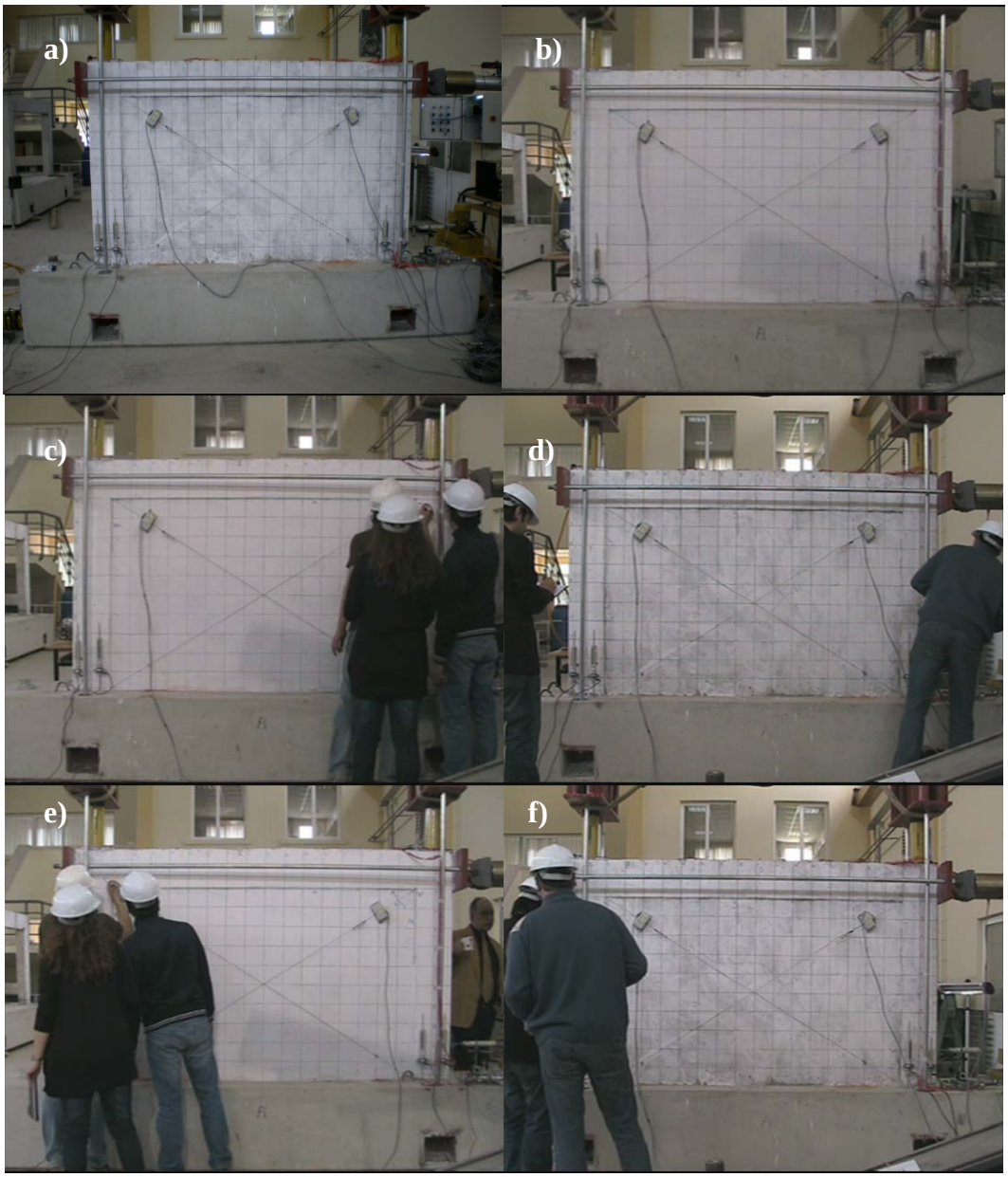

Figure 4.7 Observed damages at specific levels of drift ratio: a) Locked brick frame at the beginning of the test, b) Standard brick frame at the beginning of the test, c) Locked brick frame at 0.3% drift, d) Standard brick frame at 0.3% drift, e) Locked brick frame at -0.3% drift, f) Standard brick frame at -0.3% drift.

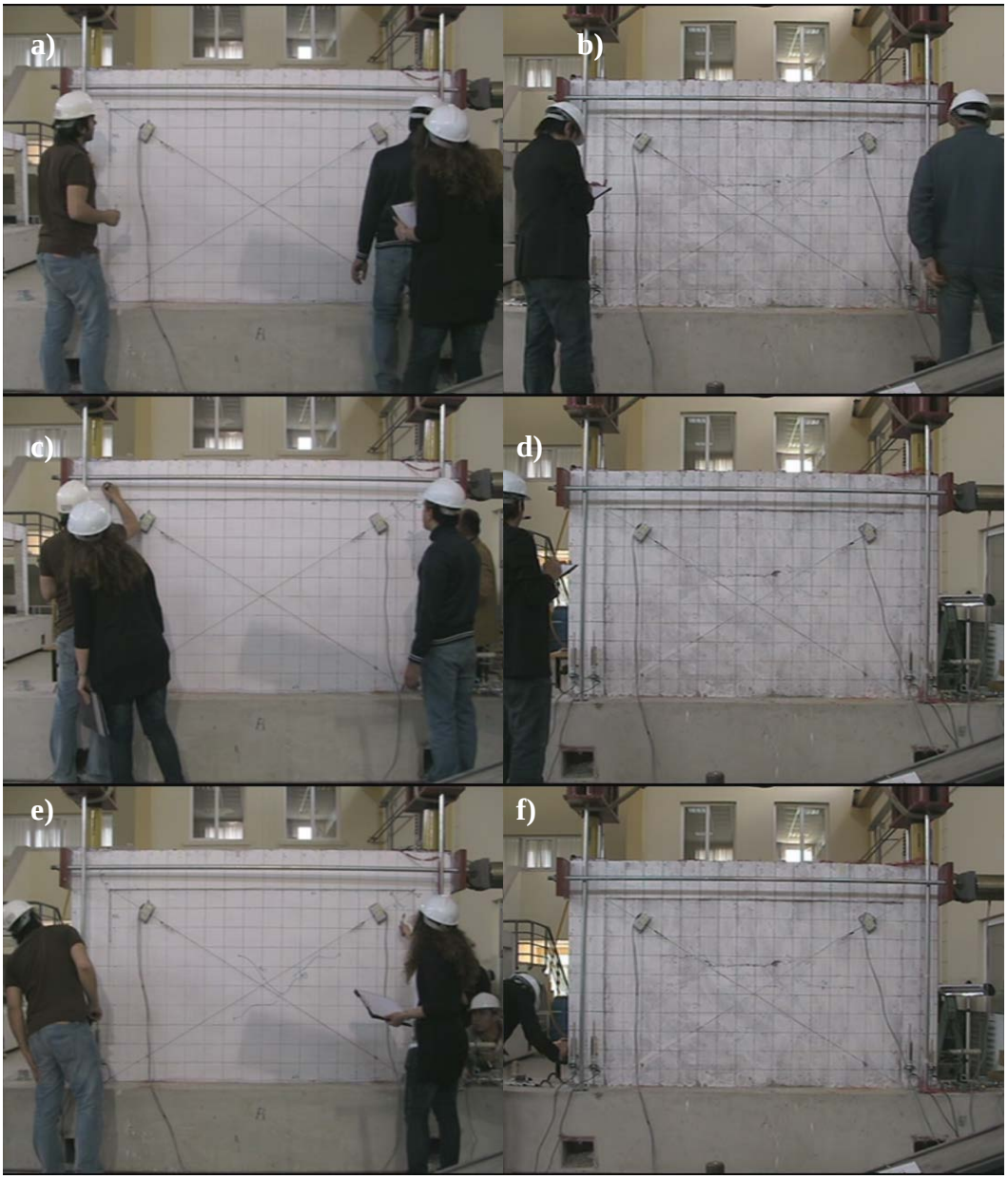

Figure 4.8 Observed damages at specific levels of drift ratio: a) Locked brick frame at 0.35% drift, b) Standard brick frame at 0.35% drift, c) Locked brick frame at -0.35% drift, d) Standard brick frame at -0.35% drift, e) Locked brick frame at 0.4% drift, f) Standard brick frame at 0.4% drift

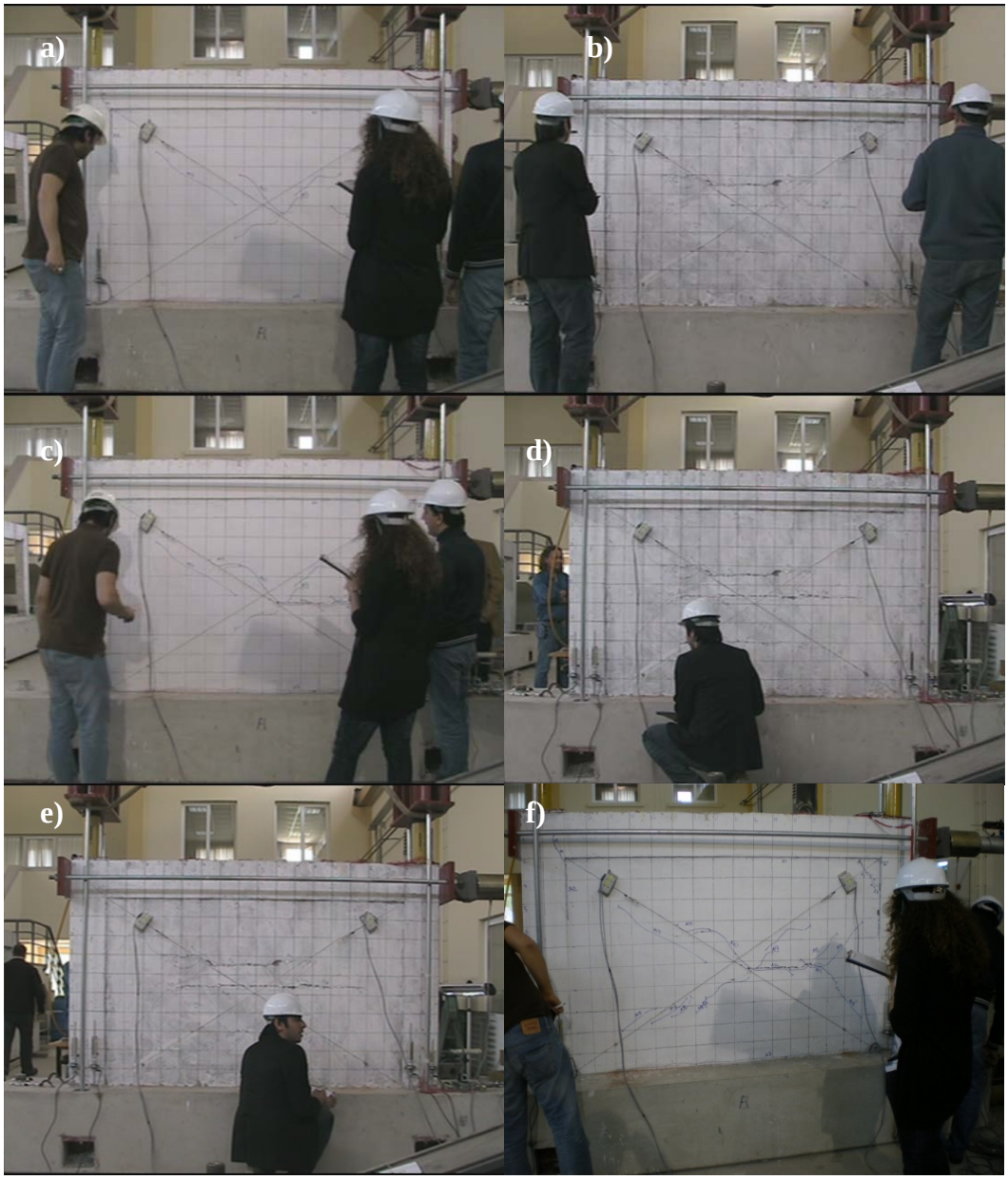

Figure 4.9 Observed damages at specific levels of drift ratio: a) Locked brick frame at -0.4% drift, b) Standard brick frame at -0.4% drift, c) Locked brick frame at 0.5% drift, d) Standard brick frame at 0.5% drift, e) Locked brick frame at -0.5% drift, f) Standard brick frame at -0.5% drift

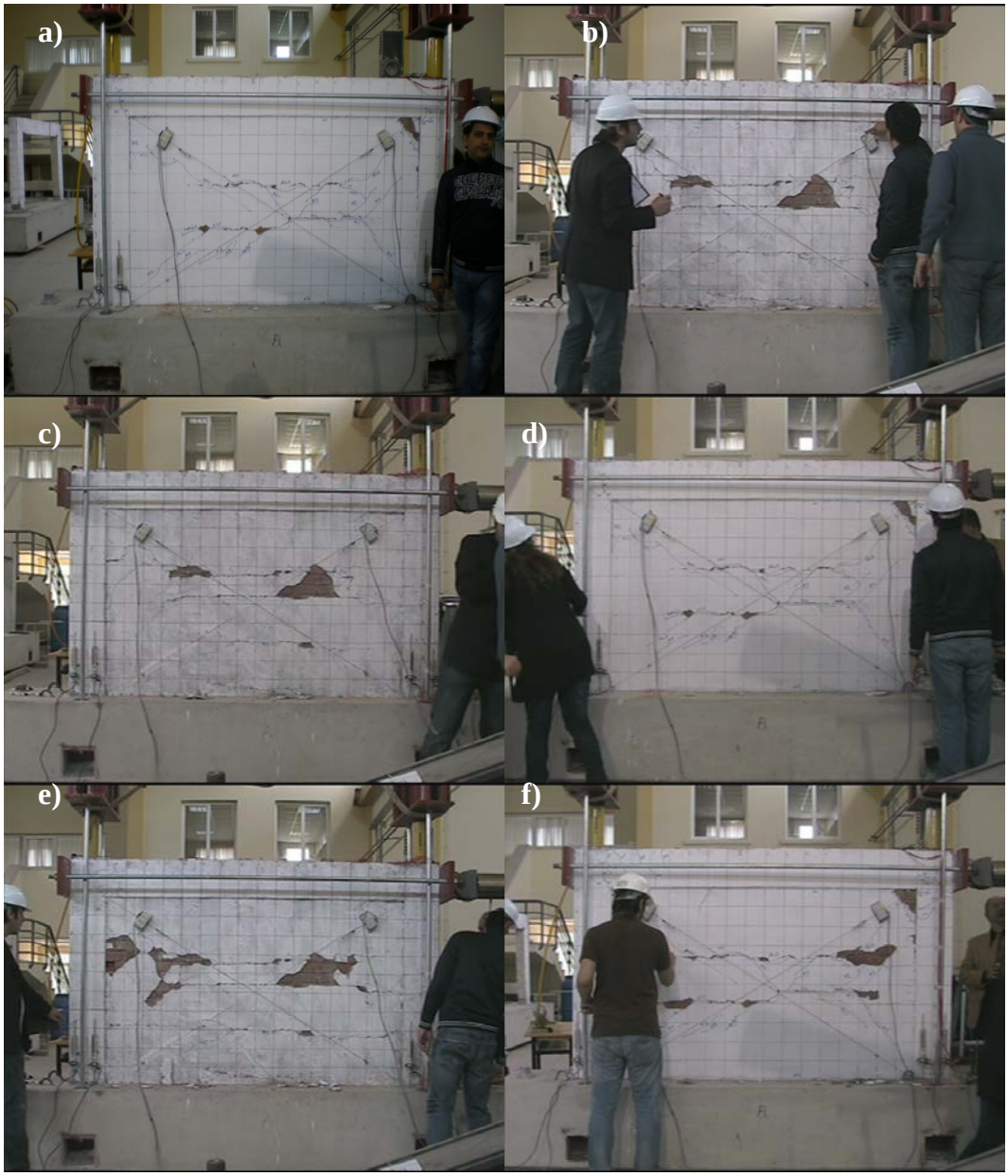

Figure 4.10 Observed damages at specific levels of drift ratio: a) Locked brick frame at 0.75% drift, b) Standard brick frame at 0.75% drift, c) Locked brick frame at -0.75% drift, d) Standard brick frame at -0.75% drift, e) Locked brick frame at 1% drift, f) Standard brick frame at 1% drift

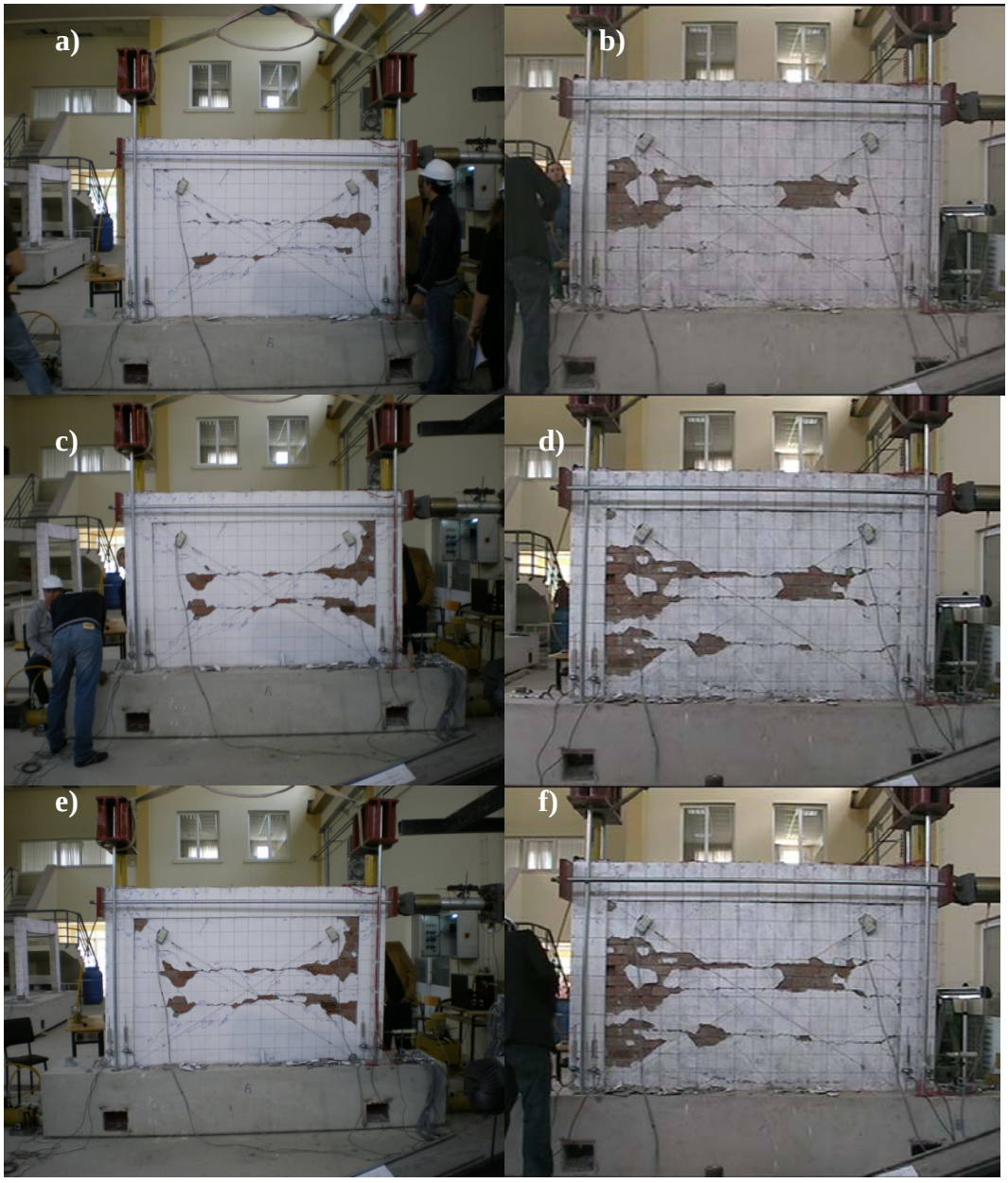

Figure 4.11 Observed damages at specific levels of drift ratio: a) Locked brick frame at -1% drift, b) Standard brick frame at -1% drift, c) Locked brick frame at 1.5% drift, d) Standard brick frame at 1.5% drift, e) Locked brick frame at -1.5% drift, f) Standard brick frame at -1.5% drift

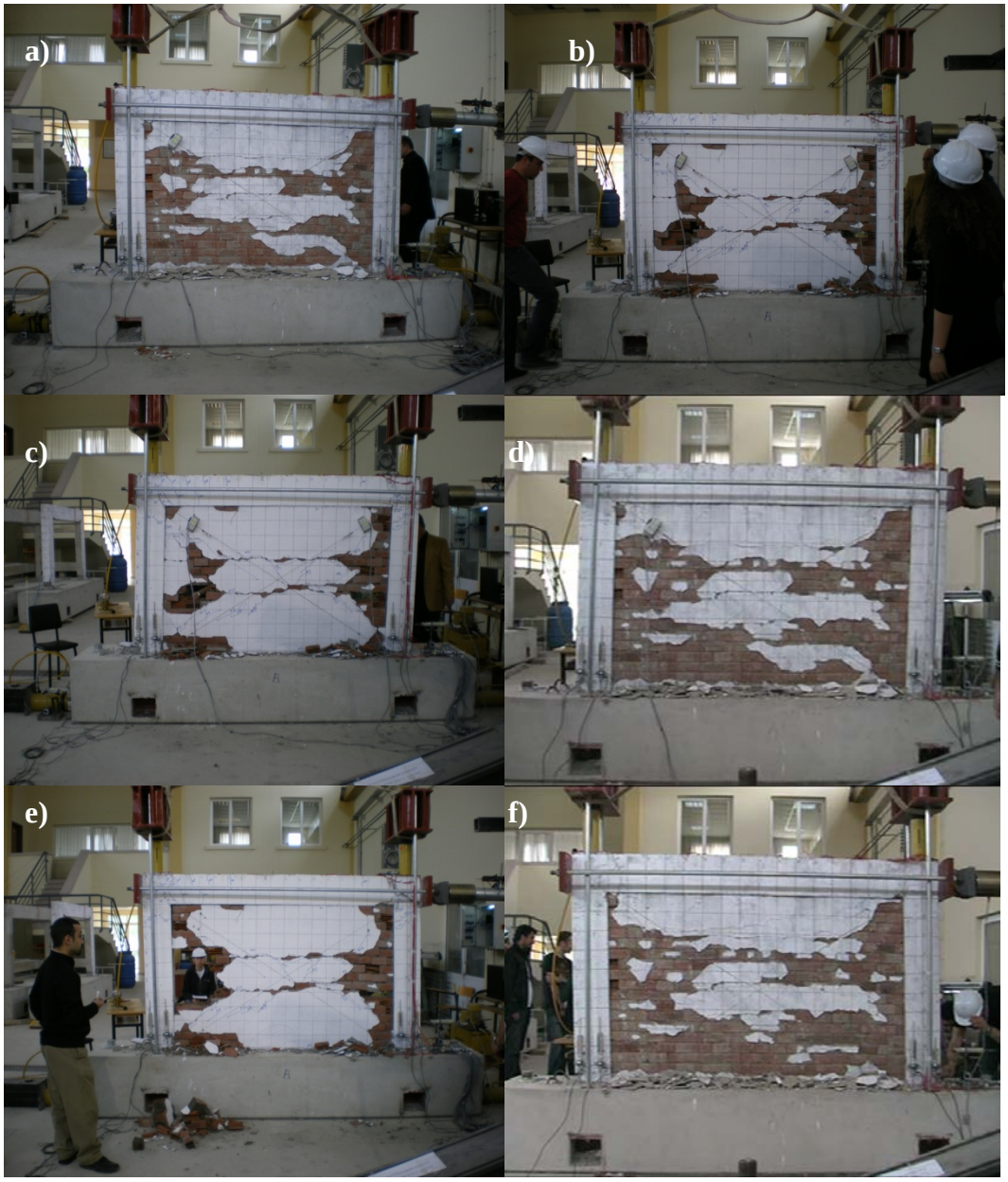

Figure 4.12 Observed damages at specific levels of drift ratio: a) Locked brick frame at 2.5% drift, b) Standard brick frame at 2.5% drift, c) Locked brick frame at -2.5% drift, d) Standard brick frame at -2.5% drift, e) Locked brick frame at 3% drift, f) Standard brick frame at 3% drift

Figure 4.13 Observed damages at specific levels of drift ratio: a) Locked brick frame at -3% drift, b) Standard brick frame at -3% drift, c) Locked brick frame at 3.5% drift, d) Standard brick frame at 3.5% drift, e) Locked brick frame at -3.5% drift, f) Standard brick frame at -3.5% drift

Figure 4.14 Observed damages at specific levels of drift ratio: a) Locked brick frame at the end of the test, b) Standard brick frame at the end of the test

CHAPTER FIVE
EVALUATION OF THE TEST RESULTS

The test results are compared with each other in terms of general behavior, strength, stiffness, cumulative damage, energy dissipation capacity, ductility, over strength, and performance factors. In addition, the advantages and disadvantages of varying infill types are discussed.

5.1 Lateral Strength and the General Behavior of the Specimens

The envelope curves of lateral load versus story drift responses obtained using test data for the bare frame, standard brick frame, and locked brick frame specimens are presented in Figure 5.1. The curves were determined by connecting intersection points of the first cycle for the i^{th} deformation step and the second cycle for the $(i-1)^{th}$ deformation step of all drift levels (Federal Emergency Management Agency [FEMA]). These plots represent the lateral strength versus lateral displacement capacities of the specimens subjected to the same displacement demand. Table 5.1 summarizes the maximum strengths values reached for the pushing and pulling directions separately, and in the same order ultimate base shear capacities are 99.5 kN, 137.1 kN, and 93.0 kN for the positive loading direction, respectively.

Table 5.1 The observed ultimate strengths (1^{st} cycle)

Specimen	Push [kN]	Pull [kN]
Bare frame	99.5	-100.0
Standard brick infilled frame	137.1	-123.4
Locked brick infilled frame	93.0	-93.4

The effect of the standard brick infill can be seen clearly. By referring to Figure 5.1 standard brick frame specimen reaches to relatively high lateral load value whereas bare frame and locked brick frame specimens have lower lateral load values, this is particularly important for the locked brick frame specimen since this frame behaves very similar in terms of lateral load capacity as the bare frame specimen. Comparison of the results for the standard brick frame specimen with the results of locked brick frame and bare frame specimens, at maximum drift ratio of 3.5% the standard brick infill walls do not increase considerably the lateral load capacity. The lateral load capacity of bare frame increases approximately 15% when standard brick

infill walls are used and almost no increase is observed in the case of locked brick frame.

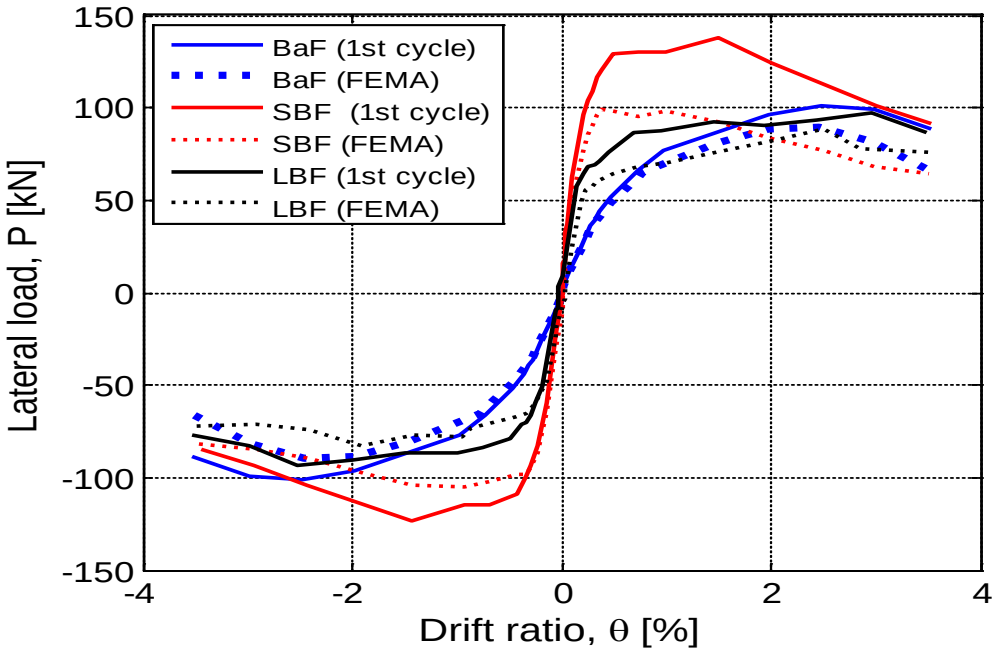

Figure 5.1 Envelope curves of bare frame, standard brick frame and locked brick frame

Two sets of envelope curves for each reinforced concrete frame case are shown in Figure 5.1. Solid lines represent the envelope curves constructed from the data recorded during the first cycle of that specific target drift level, and the dashed lines represent the envelope curves constructed using the procedure outlined in FEMA where force vs. drift ratio pairs recorded during the second cycle of that specific target drift level are used (FEMA). It should be noted here that three cycles were performed at each target drift level. Results show that infill walls deteriorate very quickly as the cycles progress within the same target drift level, and it can be concluded that infill walls exhibit extremely low ductility. It can be seen that all of the specimens reach to similar lateral load values beyond 2% drift ratio indicating that infill walls do not contribute at all to the ductility of reinforced concrete frames at high drift levels. The ductility of the infill walls are considerably low which makes it important to consider in all structural performance evaluations.

5.2 Lateral Stiffness

The peak-to-peak lateral stiffness is defined as the slope of the line connecting the positive and negative peak values of a load–displacement cycle under consideration. Variations in the lateral stiffness values with respect to story drift are calculated at the third cycle of each drift ratio (i.e., target displacement) and are plotted in Figure 5.2. As shown in Figure 5.2, the bare frame specimen constitutes the lower bound in the stiffness degradation plot. For the bare frame, standard brick frame and locked brick frame specimens, initial elastic lateral stiffnesses are 13.4 kN/mm, 71.4 kN/mm, and 39.2 kN/mm, respectively. In the elastic range, the stiffnesses of the standard brick frame and locked brick frame are 5.33 and 2.93 times larger than the corresponding stiffness of the bare frame, respectively.

The locked brick frame specimen has higher stiffness values at the early stages of the loading. A sudden drop is observed at the very beginning due to over reaching the static friction threshold and after that the stiffness starts decreasing once shear sliding starts within the infill wall and as the drift ratio increases the stiffness decreases further gradually. The lateral stiffness dropped down to 23.5 kN/mm when story drift reaches to 0.028%. After about 2.0% drift level, similar stiffness degradation can be observed in all the specimens.

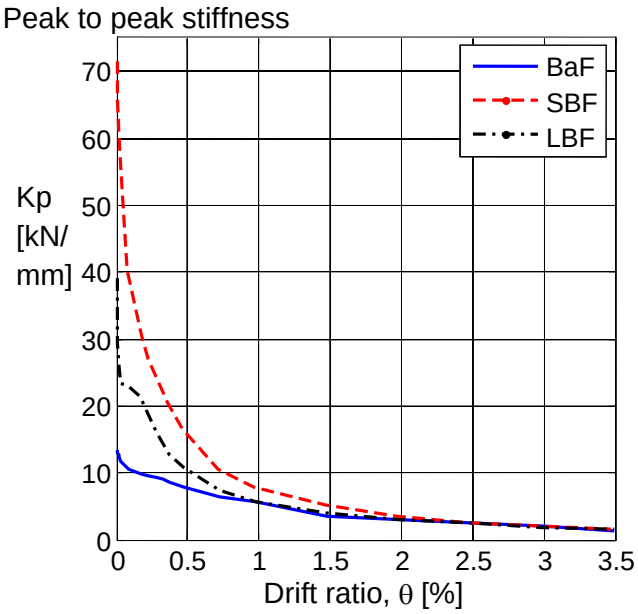

Figure 5.2 Stiffness degradation behaviour of specimens

5.3 Energy Dissipation Capacity

The ability of a structure to dissipate seismic input energy is an accurate measure of how it will perform under seismic action. The cumulative dissipated energy is defined as the sum of the area enclosed by each hysteresis loop at the same target drift level. The cumulative dissipated energy vs. story drift ratio plots are shown for all specimens in Figure 5.3**.** Discontinuities seen at target drift levels are due to having three cycles at each drift level, therefore dissipated energy accumulates with each cycle at the same drift level. The lines between the target drift levels are added to increase the readability of the plots; otherwise they do not have any physical meanings. By referring to Figure 5.3**,** it can be said that bare frame specimen has the minimum energy dissipation capacity whereas standard brick frame specimen has the highest. At 1.5% drift level where the maximum lateral load levels were reached, SBF specimen dissipates 2.78 and 1.71 times more energy than bare frame and locked brick frame specimens, respectively.

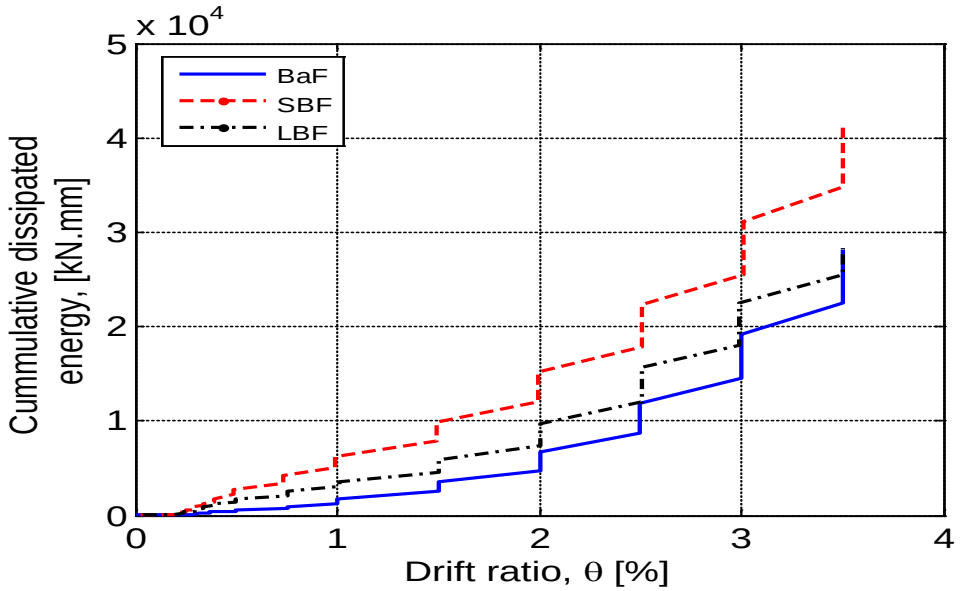

Figure 5.3 The dissipated cumulative energy vs. drift ratio plots for all specimens

CHAPTER SIX
ANALYTICAL STUDY

6.1 Introduction

Nonlinear static analyses of locked brick and standard brick infilled frames and bare frame specimen were performed under finite element software Seismostruct. The prominent features of this software are capability of predicting the large displacement behavior of space frames under static or dynamic loading, taking into account both geometric nonlinearities and material inelasticity. The axial loads which is applied to columns and quasi-static cyclic lateral loads applied to the top of the columns, modeled as in experiment.

Materials, sections, elements, restraints and loading type are the characteristics that affect specimen behavior substantially. Models (material models, element models) which related with these characteristics have numerous empirical and physical parameters.

Each specimen has an analytical model. Except for bare frame, every analytical model formed by two columns, a beam and an infill wall. Inelastic displacement-based frame elements are used for columns and beams and also inelastic infill panel element is used for infill walls. Model of an infilled frame illustrated in Figure 6.1.

The development of the analytical model is divided into two parts dealing with two components of the geometrical and material representation of the infilled frame system, namely the reinforced concrete frame and the infill wall.

6.2 Material Models

6.2.1 Concrete Model

There are 13 types of material models in Seismostruct and 7 of them are concrete models. The Mander nonlinear concrete model was chosen out of 7 concrete models. This model is a uniaxial nonlinear constant confinement model that the effects of confinement provided by the lateral transverse reinforcement. Mander et al. (1984) have proposed a unified stress-strain approach for confined concrete

applicable to both circular and rectangular shaped transverse reinforcement (Figure 6.2). In order to fully characterize the concrete model, there are five model calibrating parameters must be defined. These parameters are illustrated in Table 6.1.

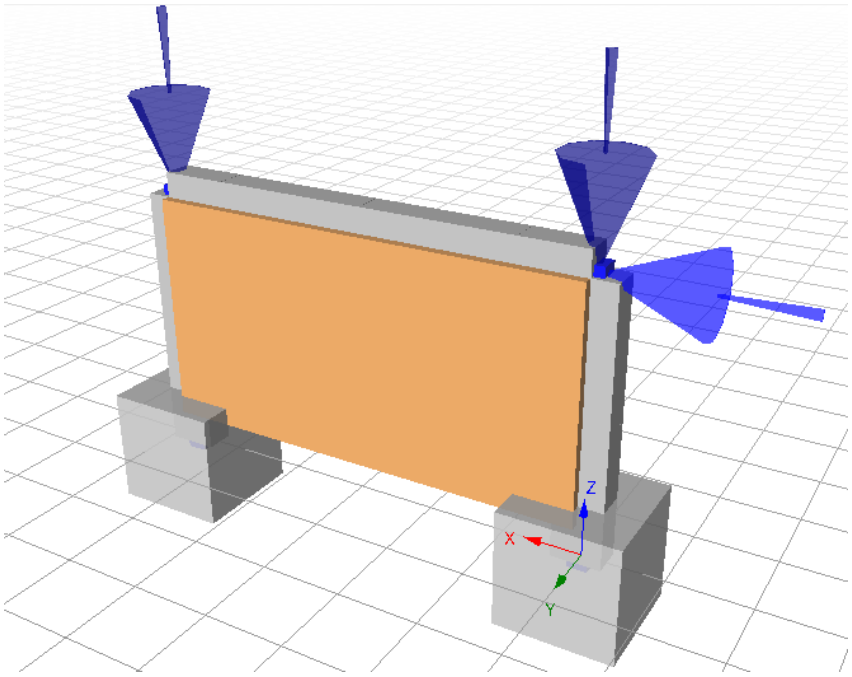

Figure 6.1 Solid model of infilled frame on Seismostruct

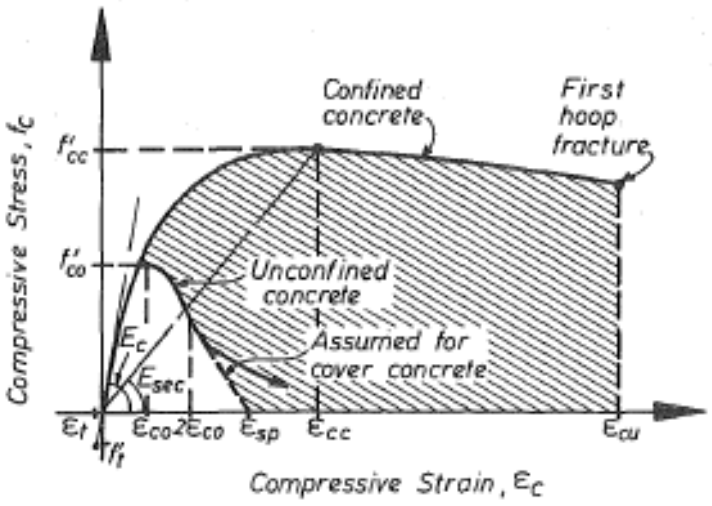

Figure 6.2 Stress-strain model proposed for monotonic loading of confined and unconfined concrete

There are two kinds of concrete model embedded to all three analytical models, one is “unconfined concrete” and the other one is “confined concrete”. The main difference between these models is confinement factor. This confinement factor is calculated with hoop dimensions and strength and area of longitudinal reinforcement bar.

Table 6.1 Model parameters of concrete model

Model Parameters	**Unconfined Concrete**	**Confined Concrete**	**Recommended Values**	**Default Value**
Compressive Strength f_c (MPa)	20	20	15-45	30
Tensile Strength – f_t (MPa)	0	0	-	0
Strain at Peak Stress – ε_c (mm/mm)	0.002	0.002	0.002-0.0022	0.002
Confinement Factor – k_c (-)	1.0	1.3	1.0-1.3	1.2
Specific Weight – γ (kN/m^3)	24	24	-	24

6.2.2 Steel Model

The Menegetto-Pinto steel model with Monti-Nuti post-elastic buckling model embedded all three analytical models. This uniaxial steel model is able to describe post-elastic behavior of reinforcing bars under compression. In order to fully characterize the steel model, there are twelve model calibrating parameters must be defined. These parameters are illustrated in Table 6.2.

Table 6.2 Model parameters of steel model

Model Parameters	Steel Model	Recommended Values	Default Value
Modulus of Elasticity – E_s (MPa)	210000	200000-210000	200000
Yield Strength – f_y (MPa)	500	230-650	500
Strain Hardening Parameter – μ (-)	0.015	0.005-0.015	0.005
Transition Curve Initial Shape Parameter – R_0 (-)	19	-	20
Transition Curve Shape Calibrating Coefficients – A1/A2 (-)	18.5/0.15	-/0.05-0.15	0.15
Kinematic/Isotropic Weighting Coefficient – P (-)	0.9	-	0.9
Spurious Unloading Corrective Parameter – r (%)	2.5	2.5-5	2.5
Transverse Reinforcement Spacing – L (mm)	50	-	200
Longitudinal Re-Bar Diameter – D (mm)	8	-	20,0
Fracture Strain – ε_{ult} (-)	0.06	-	0.1
Specific Weight – γ (kN/m^3)	78	-	78

.

6.3 Elements

6.3.1 Inelastic Displacement-Based Frame Element

Inelastic displacement-based frame element which illustrated in Figure 6.3, capable of modeling of space frames with geometric and material nonlinearities, used with displacement functions. The sectional stress-strain state of beam-column elements is obtained through the integration of the nonlinear uniaxial material response of the individual fibres in which the section has been subdivided, fully accounting for the spread of inelasticity along the member length and across the section depth.

Inelastic displacement-based frame element embedded in all analytical models as beams and columns. This element is a superposition of three fibers; Unconfined concrete fiber, confined concrete fiber and steel fibers.

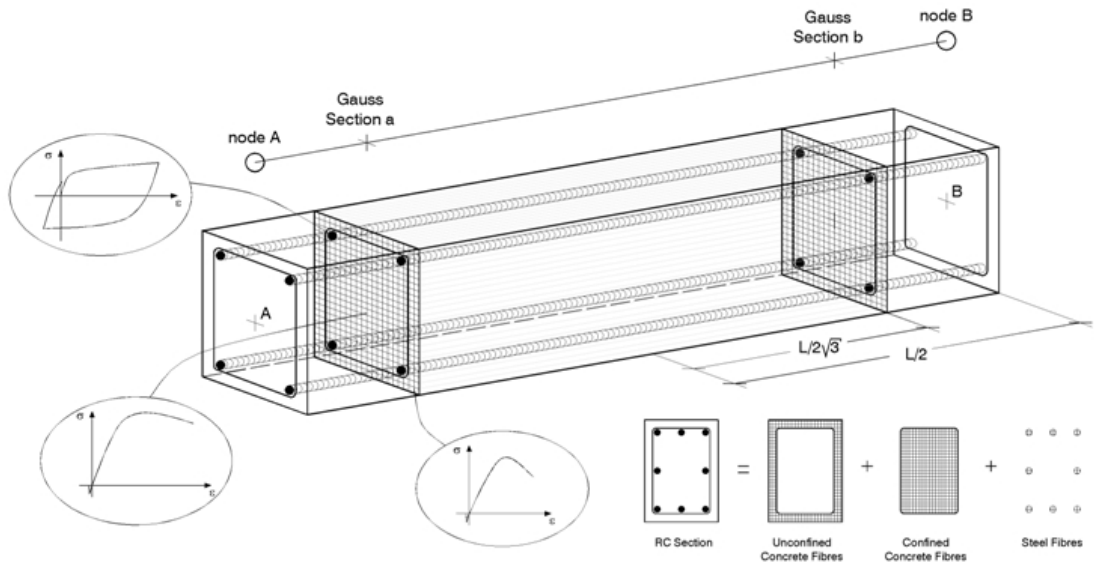

Figure 6.3 Inelastic displacement-based frame element

6.3.2 Inelastic Infill Panel Element

Each infill panel element represented by four axial struts and two shear springs, as shown in Figure 6.4. This element is able to define with three groups of parameters. First group is about physical characteristics of infill panel, second group is about compression/tension struts defined by strut curve parameters, and third group is about shear spring that defined by shear curve parameters. It is noticeable that only friction coefficients of shear strut parameter are different between standard brick frame model and locked brick frame model.

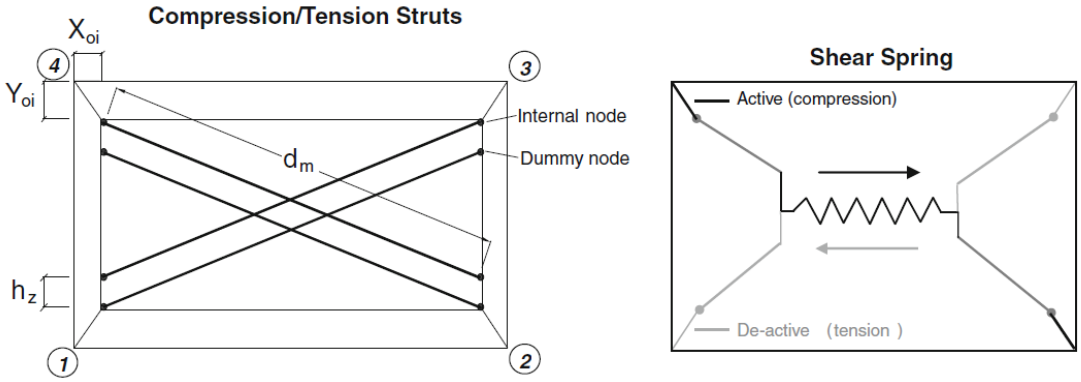

Figure 6.4 Inelastic infill panel element

Table 6.3 Infill panel parameters

Infill Panel Parameters	**Standard Brick**	**Locked Brick**	**Recommended Values**	**Default Value**
Panel Thickness – t (mm)	145	150	-	50
Out-of-Plane Failure Drift (%)	5	5	-	5
Strut Area 1 – A_1 (mm^2)	44685	44685	-	30000
Strut Area 2 – A_2 (%)	50	50	-	40
Equivalent Contact Length – h_z (%)	23	23	-	23
Horizontal Offset – x_0 (%)	2.4	2.4	-	2.4
Vertical Offset – y_0 (%)	10	10	-	10
Proportion of Stiffness Assigned to Shear – γ_s (%)	60	60	-	20
Specific Weight – γ (kN/m^3)	10^{-8}	10^{-8}	-	10

Table 6.4 Strut curve parameters

Strut Curve Parameters	**Standard Brick**	**Locked Brick**	**Recommended Values**	**Default Value**
Initial Young Modulus – E_m (MPa)	700	700	-	1600
Compressive Strength – $f_{m\Theta}$ (MPa)	1.1	1.1	-	1
Tensile Strength – f_t (MPa)	0	0	-	0.575
Strain at Maximum Stress – e_m (mm/mm)	0.0012	0.0012	-	0.0012
Ultimate Strain – ε_{ult} (mm/mm)	0.015	0.015	-	0.024
Closing Strain – ε_{cl} (mm/mm)	0.004	0.004	0-0.003	0.004
Strut Area Reduction Strain – ε_1 (-)	0.006	0.006	0.003-0.008	0.006
Residual Strut Area Strain – ε_2 (-)	0.0006	0.0006	0.0006-0.016	0.0006
Starting Unloading Stiffness Factor – γ_{un} (-)	1.5	1.5	1.5-2.5	1.5
Strain Reloading Factor - $\propto_{re}$ (-)	0.2	0.2	0.2-0.4	0.2
Strain Inflection Factor - $\propto_{ch}$ (-)	0.7	0.7	0.1-0.7	0.7
Complete Unloading Strain Factor – β_a (-)	1.5	1.5	1.5-2.0	1.5
Stress Inflection Factor – β_{ch} (-)	0.9	0.9	0.5	0.9
Zero Stress Stiffness Factor – γ_{plu} (-)	1	1	0-1	1
Reloading Stiffness Factor – γ_{plr} (-)	1.1	1.1	1.1-1.5	1.1

Plastic Unloading Stiffness Factor – e_{x1} (-)	3	3	1.5-3	3
Repeated Cycle Strain Factor - e_{x2} (-)	1.4	1.4	1-1.5	1.4

Table 6.5 Shear curve parameters

Shear Curve Parameters	**Standard Brick**	**Locked Brick**	**Recommended Values**	**Default Value**
Shear Bond Strength – τ_0 (MPa)	1.5	1.5	0.1-1.5	0.3
Friction Coefficient – μ (-)	0.7	0.1	0.1-1.2	0.3
Maximum Shear Strength – τ_{max} (MPa)	1.6	1.6	-	0.6
Reduction Shear Factor - $\propto_s$	1.5	1.5	1.4-1.65	1.5

6.4 Analysis Results

6.4.1 Bare Frame

The pinching behavior which is shown experimental results of bare frame, is unsatisfactory at analytical model. The comparison of analytical Seismostruct model and experimental test results is illustrated Figure 6.5. The figure depicted both analytical and experimental base shear roof drift ratio graphs.

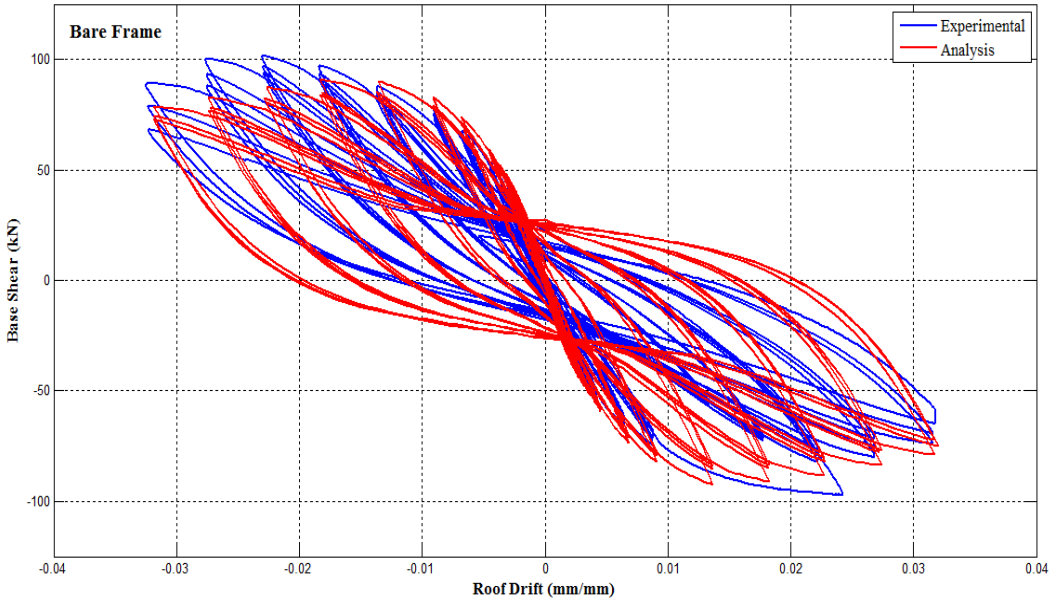

Figure 6.5 Analytical and experimental hysteretic behavior of bare frame

6.4.2 Standard Brick Frame

The comparison of analytical Seismostruct model and experimental test results is illustrated Figure 6.6. The figure depicted both analytical and experimental base shear roof drift ratio graphs.

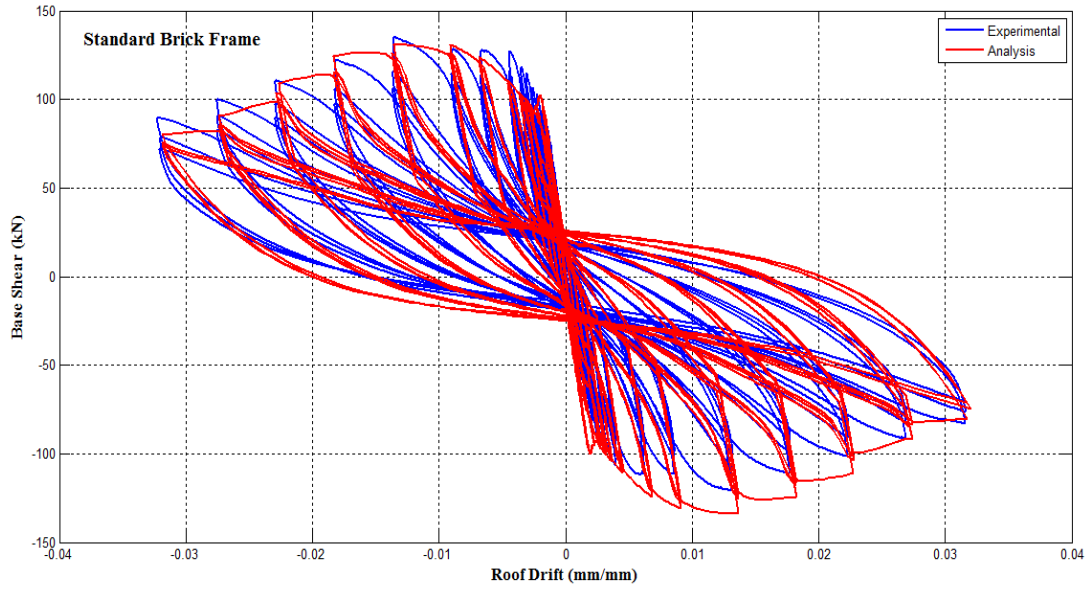

Figure 6.6 Analytical and experimental hysteretic behavior of standard brick frame

6.4.3 Locked Brick Frame

The comparison of analytical Seismostruct model and experimental test results is illustrated Figure 6.7. The figure depicted both analytical and experimental base shear roof drift ratio graphs.

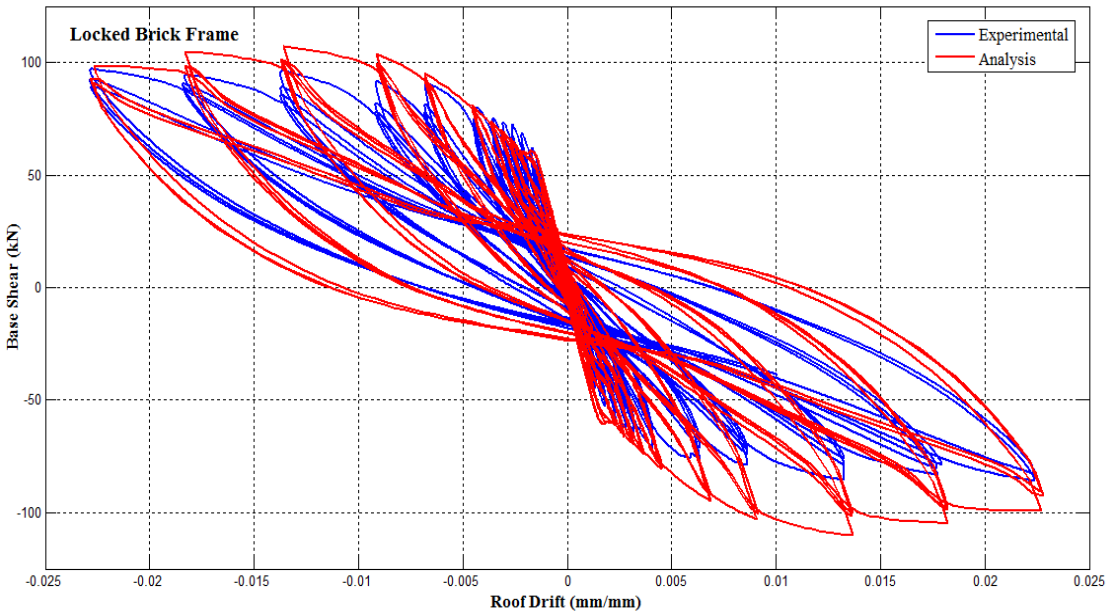

Figure 6.7 Analytical and experimental hysteretic behavior of standard brick frame

CHAPTER SEVEN
CONCLUSIONS

In this study, three one bay-one storey reinforced concrete frames with different masonry infill wall conditions are tested under cyclic loading. Results are presented in terms of force – interstory drift ratio, stiffness degradation, and cumulative energy dissipation ratio plots and comparisons are made.

The presence of masonry infill walls affects the seismic behavior of framed building to large extent. These effects are generally positive based on the type of masonry infill wall used. Masonry infill walls increase global stiffness and strength of the structure. It is observed that

i. Standard brick infill walls do not increase the lateral load capacity of reinforced concrete frames considerably within the results of FEMA procedure. The lateral load capacity of bare frame increases approximately 15% with standard brick infilled frames and almost no increase is observed when locked brick infilled frames are used.

ii. Since the ductility of the standard brick infill wall is very low, lateral resistance contribution of this infill wall is almost negligible at high drift levels. For the locked brick infill wall, since the wall is free to deform with the frame, lateral strength do not change considerably. For all the specimens, similar story shear values are observed beyond 2% drift ratio.

iii. Infill walls in general are not taken into account during the modeling phase of the structures, but it is a well known fact that they change the dynamic characteristics of the structures; in this study it is shown that the locked brick infill walls change the initial lateral stiffness of the structure much less than the standard infill walls, therefore the modeled and the real structure will be more similar in terms of their dynamic characteristics, and the design will be more reliable.

iv. Locked brick infill walls change the lateral stiffness of reinforced concrete frames considerably less compare to the standard infill walls; this attribute of the locked bricks has the potential in reducing the negative effects of vertical and lateral stiffness irregularities in structures caused by irregular layout of infill walls at

different story levels.

v. The cumulative energy dissipation capacity of the frames with both types of infill walls is higher than that of the bare frame. But this is due to reaching higher levels of lateral forces. At higher drift levels, energy dissipation capacities for three different frames are similar.

vi. Locked brick infill walls maintained their integrity up to very high drift levels (i.e., 3% and beyond), this opens the possibility of using this type of bricks for increasing the viscous damping levels of reinforced concrete type structures by adding a special viscous material at the sliding interfaces.

vii. Locked brick infill walls preserved their in-plane stability from the start till the end of the test; indicating that the locked infill walls have an improved behavior of out-of-plane stability compare to the standard ones. This may prove useful during a multi-axial earthquake shaking by lowering falling hazards of infill walls on people and therefore decreasing injuries and fatalities.

REFERENCES

ACI Innovation Task Group 1 and Collaborators (2001) *Commentary on Acceptance Criteria for Moment Frames Based on Structural Testing.* Farmington Hills: American Concrete Instute.

Aref, J.A. & Jung, W.Y. (2003). Energy dissipating polymer matrix composite-infill wall system for seismic retrofitting. *Journal of Structural Engineering, 129(4),* 440-448.

Coope, M. (n.d.). *The Strain Gauge.* Retrieved September 7, 2011, from http://www.sensorland.com/HowPage002.html.

Crisafulli, F.J., Carr, A.J. & Park, R. (2000). Capacity design of infilled frame structures. *12th World Conference on Earthquake Engineering*.

D'Ayala, D., Worth, J. & Riddle, O. (2009). Realistic shear capacity assessment of infill frames: comparison of two numerical procedures. *Engineering Structures, 31,* 1745-1761.

Federal Emergency Management Agency - 306 (1999). *Evaluation of earthquake damaged concrete and masonry wall buildings –Basic procedures manual. Federal Emergency Management Agency*.

Gülkan, P., Wasti, S.T. 1993 Frame-Infill Interaction: A Non-linear investigation. *12 th Technical Congress in Civil Engineering.*

Holmes, M. (1961). Steel frames with brickwork and concrete infilling. *Institution of Civil Engineers Proceedings, 19(4),* 473-478

Klingner, R.E. & Bertero, V.V. (1976). Infilled frames in earthquake-resistant construction. *Rep. EERC 76-32, University of California.*

Marjani, F. & Ersoy, U. (2002). Behavior of brick infilled reinforced concrete frames under reversed cyclic loading. *ECAS2002 International Symposium on Structural and Earthquake Engineering*, 142-150.

Mallick, D.V. & Severn, R.T. (1967). The behaviour of infilled frames under static loading. *Institution of Civil Engineers Proceedings, 38(2),* 639-656.

Mehrabi, A.B., Shing, P.B, Schuller, M.P. & Noland J.L. (1996). Experimental evaluation of masonry-infilled reinforced concrete frames. *Journal of Structural Engineering, 122(3),* 228-237.

Ministry of Public Works and Settlement. (2007). Specification for Structures to be Built in Disaster Areas. *IMO/09/01*.

Mohammadi, M. & Akrami, V. (2010). An engineered infilled frame: behavior and calibration. *Journal of Constructional Steel Research, 66,* 842-849.

Moghadam, H.A. (2004). Lateral load behavior of masonry infilled steel frames with repair and retrofit. *Journal of Structural Engineering, 130(1),* 56-63.

Mosalam, K.M., White, R.M. & Gergely, P. (1997). Static response of infilled frames using quasi-static experimentation. *Journal of Structural Engineering, 123(11),* 1462-1469.

Sahota, M. K. & Riddington, J.D. (2001). Experimental investigation into using lead to reduce vertical load transfer in infilled frames. *Engineering Structures, 23(1),* 94-101.

Seismosoft. (2002). *Seismostruct Version 5.2.2* Retrieved September 25, 2011 from http://www.seismosoft.com

Taher, S.F. & Afefy, H.M. (2008). Roll of the masonry infill on seismic resistance of RC structure. *Arabian Journal for Science and Engineering, 33(2B),* 261-306.